

# SUB-GAP TRANSPORT IN SUPERCONDUCTOR-DOT JUNCTIONS

Master thesis by  
Anika Haller

Supervisor:  
Prof. Jens Paaske  
Prof. Felix von Oppen

April 22, 2014



DEPARTMENT OF PHYSICS  
FREIE UNIVERSITÄT BERLIN  
ARNIMALLEE 14  
14195 BERLIN, GERMANY



# Contents

<b>1</b>	<b>Introduction</b>	<b>5</b>
<b>2</b>	<b>Superconductivity</b>	<b>6</b>
2.1	The BCS ground state . . . . .	6
2.2	The BCS mean-field Hamiltonian . . . . .	7
2.3	Superconductor—normal-metal interfaces . . . . .	8
<b>3</b>	<b>Green functions</b>	<b>10</b>
3.1	Green functions for many-body systems . . . . .	11
3.2	Equation of motion theory . . . . .	13
3.3	The Lehmann representation . . . . .	14
3.3.1	Lesser and greater Green function . . . . .	14
3.3.2	Retarded and advanced Green function . . . . .	15
3.3.3	Spectral function . . . . .	16
3.4	Imaginary-time Green functions . . . . .	18
3.4.1	Fourier transform of Matsubara Green functions . . . . .	18
3.4.2	Equation of motion for Matsubara Green functions . . . . .	19
3.4.3	Connection between Matsubara and retarded Green function . . . . .	20
3.5	Contour ordered Green functions . . . . .	20
<b>4</b>	<b>Transport in superconductor —quantum-dot junctions</b>	<b>23</b>
4.1	Model Hamiltonian . . . . .	23
4.1.1	Nambu representation . . . . .	24
4.2	The system’s Green functions . . . . .	26
4.2.1	Matsubara Green function for the leads . . . . .	26
4.2.2	Hybridization Matsubara Green function . . . . .	27
4.2.3	Matsubara Green function for the dot . . . . .	28
4.2.4	Retarded and advanced Green functions . . . . .	30
4.3	Derivation of the current . . . . .	32
4.4	The one-level dot system . . . . .	36
4.4.1	Spectral function and Andreev bound states . . . . .	36
4.4.2	The current . . . . .	44
4.4.3	Zeeman-split dot levels . . . . .	53
<b>5</b>	<b>Summary &amp; Outlook</b>	<b>57</b>
<b>6</b>	<b>Acknowledgements</b>	<b>59</b>
<b>A</b>	<b>Fourier transformation</b>	<b>61</b>
	<b>References</b>	<b>62</b>



# 1 Introduction

The quantum transport in systems of quantum-dots (QD) connected to reservoirs in the superconducting state (S) is of great interest in condensed matter physics. For example, in [1] they measure the spectrum of a segment of InAs nanowire, confined between two superconducting leads. One would like to understand the fundamental principles of the transport properties of those S-QD-S systems to derive potential applications for nanoelectronics. Thereby, the quantum-dot is a confined region of atomic size, that can be used to control the current through the system. This combination of nanostructures with objects of  $\mu m$ -size are also called mesoscopic systems.

The systems of interest can be of different structure and properties. There are a lot of considerations especially for the properties of the dot. There have been studies, e.g., on multilevel quantum dots [2, 3], where they consider spin-orbit coupling between the levels among other things. Furthermore, one considers dots with local Coulomb repulsion or level splitting caused by the Zeeman effect [4]. There are as well studies on S-QD systems that are additionally coupled to a normal metal (N).

As superconductors are very sensitive to magnetic impurities, one is also interested in dots that describe single quantum-spin impurities [1]. The exchange interaction with the quasiparticles of the superconductor give rise to the so-called Yu-Shiba-Rusinov sup-gap states [5].

If one talks about the current in S-QD-S systems, one is often interested in the so-called supercurrent, which is a current that exists without any bias voltage. It is caused by the phase difference between weakly coupled superconductors, whereby the phases in the superconductors are caused by an external magnetic field.

We would like to understand the transport principles for those superconductor/quantum-dot systems. Therefore, we are going to consider the special case of a noninteracting one-level dot coupled to a superconducting lead on each side. This is probably the most simple system we can think of, but all other systems can be built up on the basis of this resonant level system.

We introduce the BCS-theory of superconductivity and the theory of Green functions first. Then we derive the Green functions and the supercurrent. We find general formulas for a non-interacting multi-level dot coupled to an arbitrary number of leads. We then do numerical calculations for the special case of only one dot level (spin-degenerate) coupled to two leads, where we calculate the supercurrent and the bound state current. We compare this to the work of [6]. Furthermore, we study the influence of an additional normal lead and Zeeman splitting on the supercurrent and the spectral function.

## 2 Superconductivity

Below a critical temperature  $T_c$  some metals go over into the superconducting phase. Thereby, the electrical resistance vanishes and magnetic fields below a critical value are expelled completely. The quasiparticles in superconductors behave differently than in normal metals.

Here, we will introduce the microscopic theory of superconductivity, which is explained by the Bardeen-Cooper-Schrieffer (BCS) theory. We will explicitly have a look at interfaces of superconductors and normal metals. This section is based on the explanations in [7–9].

### 2.1 The BCS ground state

To get to the superconducting ground state, let us start from a homogeneous non-interacting electron gas, where low-energy electronic excitations are determined by the momentum  $\mathbf{k}$  and mass  $m$  of the electron as well as the chemical potential  $\mu$ , as they are of energy  $\mathbf{k}^2/2m - \mu$ . When we turn on the electron-electron interaction, these electronic excitations turn into the so-called quasiparticle excitations of equal momenta but different energy  $\xi_{\mathbf{k}}$ . At last, we get the influence of phonons, which mediate an attractive interaction between pairs of quasiparticles. These are known as *Cooper-pairs*. The effective phonon-mediated interaction is attractive as long as for the quasiparticle energy it is  $|\xi_{\mathbf{k}}| < \omega_D$ . Otherwise, the interaction is zero. Here,  $\omega_D$  is the Debye-energy, which is the maximum phonon energy in the Debye model. Since the Debye-energy is much smaller than the Fermi-energy  $\varepsilon_F$ , it must be  $|\xi_{\mathbf{k}}| \ll \varepsilon_F$ . Note that  $\xi_{\mathbf{k}}$  is measured from the Fermi surface. Conclusively, the formation of Cooper-pairs is close to the Fermi surface. The superposition of states built up of Cooper-pairs gives the superconducting ground state.

The BCS-Hamiltonian describes the interaction of the electrons in the superconductor,

$$H_{\text{BCS}} = \sum_{\mathbf{k}\sigma} \xi_{\mathbf{k}} c_{\mathbf{k}\sigma}^\dagger c_{\mathbf{k}\sigma} + \sum_{\mathbf{k}\mathbf{k}'} V_{\mathbf{k}\mathbf{k}'} c_{\mathbf{k}\uparrow}^\dagger c_{-\mathbf{k}\downarrow}^\dagger c_{-\mathbf{k}'\downarrow} c_{\mathbf{k}'\uparrow}, \quad (2.1)$$

with the attractive coupling strength

$$V_{\mathbf{k}\mathbf{k}'} = \begin{cases} -V < 0, & \text{for } |\xi_{\mathbf{k}}|, |\xi_{\mathbf{k}'}| < \omega_D, \\ 0, & \text{otherwise.} \end{cases} \quad (2.2)$$

The quasiparticle operators  $c_{\mathbf{k}\sigma}^\dagger, c_{\mathbf{k}\sigma}$  create or annihilate fermionic particles with momentum  $\mathbf{k}$  and spin  $\sigma = \uparrow, \downarrow$ . They obey the anti-commutation relations,

$$\{c_{\mathbf{k}\sigma}, c_{\mathbf{k}'\sigma'}\} = 0, \quad \{c_{\mathbf{k}\sigma}^\dagger, c_{\mathbf{k}'\sigma'}^\dagger\} = 0, \quad \{c_{\mathbf{k}\sigma}, c_{\mathbf{k}'\sigma'}^\dagger\} = \delta_{\mathbf{k}\mathbf{k}'} \delta_{\sigma\sigma'}, \quad (2.3)$$

where the anti-commutator of two operators  $A$  and  $B$  is defined as  $\{A, B\} = AB - BA$ .

## 2.2 The BCS mean-field Hamiltonian

In many-body problems it is often convenient to do approximations that lead to an effective single particle problem. The motion of interacting particles is usually correlated and therefore too complicated to be treated independently.

In the mean-field theory a single particle interacts with the average field of the other particles. In this theory one usually makes the assumption that the density operator deviates only little from its average value. In the BCS theory they assume the average value of the pair operator  $\langle c_{\mathbf{k}\uparrow}^\dagger c_{-\mathbf{k}\downarrow}^\dagger \rangle$  to be non-zero for temperatures below  $T_c$ . The fluctuations of the pair operator around its average value is assumed to be small. Here, we define the deviation operators,

$$\delta_{\mathbf{k}}^\dagger = c_{\mathbf{k}\uparrow}^\dagger c_{-\mathbf{k}\downarrow}^\dagger - \langle c_{\mathbf{k}\uparrow}^\dagger c_{-\mathbf{k}\downarrow}^\dagger \rangle, \quad \delta_{\mathbf{k}} = c_{-\mathbf{k}\downarrow} c_{\mathbf{k}\uparrow} - \langle c_{-\mathbf{k}\downarrow} c_{\mathbf{k}\uparrow} \rangle. \quad (2.4)$$

Thus, it is

$$c_{\mathbf{k}\uparrow}^\dagger c_{-\mathbf{k}\downarrow}^\dagger = \delta_{\mathbf{k}}^\dagger + \langle c_{\mathbf{k}\uparrow}^\dagger c_{-\mathbf{k}\downarrow}^\dagger \rangle, \quad c_{-\mathbf{k}\downarrow} c_{\mathbf{k}\uparrow} = \delta_{\mathbf{k}} + \langle c_{-\mathbf{k}\downarrow} c_{\mathbf{k}\uparrow} \rangle. \quad (2.5)$$

Now, we can rewrite the Hamiltonian, Eq. (2.1), in terms of the deviation operators,

$$H_{\text{BCS}} = \sum_{\mathbf{k}\sigma} \xi_{\mathbf{k}} c_{\mathbf{k}\sigma}^\dagger c_{\mathbf{k}\sigma} + \sum_{\mathbf{k}\mathbf{k}'} V_{\mathbf{k}\mathbf{k}'} \left[ \delta_{\mathbf{k}}^\dagger \delta_{\mathbf{k}'} + \delta_{\mathbf{k}'} \langle c_{\mathbf{k}\uparrow}^\dagger c_{-\mathbf{k}\downarrow}^\dagger \rangle + \delta_{\mathbf{k}}^\dagger \langle c_{-\mathbf{k}'\downarrow} c_{\mathbf{k}'\uparrow} \rangle + \langle c_{\mathbf{k}\uparrow}^\dagger c_{-\mathbf{k}\downarrow}^\dagger \rangle \langle c_{-\mathbf{k}'\downarrow} c_{\mathbf{k}'\uparrow} \rangle \right]. \quad (2.6)$$

As the deviations are small, the term  $\sum_{\mathbf{k}\mathbf{k}'} V_{\mathbf{k}\mathbf{k}'} \delta_{\mathbf{k}}^\dagger \delta_{\mathbf{k}'}$  can be neglected. Then we plug the definitions for the deviation operators back in the Hamiltonian. Thus, we obtain the mean-field BCS Hamiltonian,

$$H_{\text{BCS}}^{\text{MF}} = \sum_{\mathbf{k}\sigma} \xi_{\mathbf{k}} c_{\mathbf{k}\sigma}^\dagger c_{\mathbf{k}\sigma} - \sum_{\mathbf{k}} \Delta_{\mathbf{k}} c_{\mathbf{k}\uparrow}^\dagger c_{-\mathbf{k}\downarrow}^\dagger - \sum_{\mathbf{k}} \Delta_{\mathbf{k}}^* c_{-\mathbf{k}\downarrow} c_{\mathbf{k}\uparrow}. \quad (2.7)$$

Here, we used that  $V_{\mathbf{k}\mathbf{k}'} = V_{\mathbf{k}'\mathbf{k}}^*$  and introduced the mean-field parameter,

$$\Delta_{\mathbf{k}} = - \sum_{\mathbf{k}'} V_{\mathbf{k}\mathbf{k}'} \langle c_{-\mathbf{k}'\downarrow} c_{\mathbf{k}'\uparrow} \rangle. \quad (2.8)$$

The constant term,  $-\sum_{\mathbf{k}\mathbf{k}'} V_{\mathbf{k}\mathbf{k}'} \langle c_{\mathbf{k}\uparrow}^\dagger c_{-\mathbf{k}\downarrow}^\dagger \rangle \langle c_{-\mathbf{k}'\downarrow} c_{\mathbf{k}'\uparrow} \rangle$ , has been absorbed into the chemical potential.

The quasiparticle excitation spectrum for the BCS superconductor is found in terms of the so-called Bogoliubov transformation, which we will not get into here, but it is found as

$$E_{\mathbf{k}} = \sqrt{\xi_{\mathbf{k}}^2 + |\Delta_{\mathbf{k}}|^2}. \quad (2.9)$$

It is the energy, that is required to create a quasiparticle of momentum  $\mathbf{k}$  in the superconducting state. The energy  $E_{\mathbf{k}}$  differs from the excitation spectrum of a quasiparticle in a normal metal in the vicinity of the Fermi surface, Fig. 1. There, an energy gap opens up due to the mean-field parameter  $\Delta_{\mathbf{k}}$ , which is therefore also called the *energy-gap* parameter. The quasiparticles in the superconductor thus have a minimum energy of  $|\Delta_{\mathbf{k}_F}| = |\Delta_0|$ .

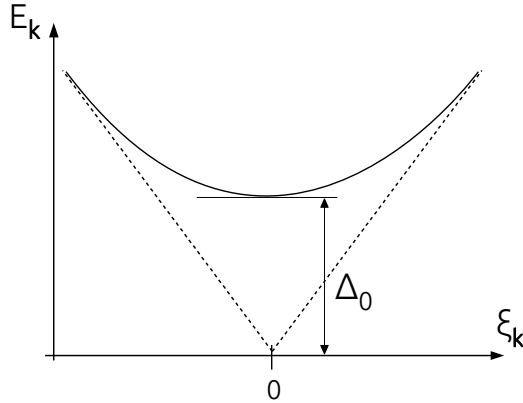


**Figure 1:** Quasiparticle spectrum of the superconductor (solid line) compared to that of a normal metal (dashed line) close to the Fermi surface. Remember that  $\xi_{\mathbf{k}}$  is measured from the Fermi level. A quasiparticle excitation in a superconductor has a minimum energy of  $\Delta_0$ .

### 2.3 Superconductor—normal-metal interfaces

Since this thesis is about superconductor-dot junctions, we will have a closer look at the properties of an interface of a superconductor (S) and a normal metal (N), see Fig. 2. The electrons in N are assumed to be noninteracting. An electron with energy  $E_{\mathbf{k}} \geq \Delta_0$  can freely propagate from N to S, where it will be converted into a quasiparticle of different momentum, but same energy. Since there are no excitations in S with energies smaller than  $\Delta_0$ , an electron coming from N with an energy below  $\Delta_0$  will be reflected. In some cases it is reflected as a hole, which almost moves into opposite direction of the incident electron. This results in a charge deficit of  $2e$  in N. The missing charge is explained by the addition of a Cooper-pair of charge  $2e$  to the superconductor. This scattering process is called *Andreev reflection*. It can run backwards as well, which means a hole in N is reflected back from S as an electron, which causes the removal of a Cooper-pair from S. We note, electrons with energies below  $\Delta_0$  can only be absorbed or emitted in pairs by the superconductor.

Consider N being a nanostructure, i.e., an object of  $nm$ -size which gives rise to discrete energy levels. Then we put N between two superconductors  $S_L$  and  $S_R$  of different phases, without any bias voltage, see Fig. 3. An electron in the nanostructure with energy lower than  $\Delta_0$  can be Andreev reflected several times between the interfaces of the two superconductors. This means, the electron is reflected back as a hole from one of the superconductors, then the hole moves towards the other superconductor and is reflected back as an electron again, and so on. Conclusively, the electron/hole in N must perform a finite motion, which gives rise to discrete energy levels. These are the so-called *Andreev bound states*. There is an Andreev bound state for each level in the nanostructure. The bound states depend on the phase difference between  $S_L$  and  $S_R$  and the level energy in N.

Every time an electron is reflected back as a hole, a Cooper pair has been added to the superconductor. If the hole then moves towards the other superconductor it will be reflected back as an electron and thereby remove a Cooper pair. Then the electron moves again towards the first superconductor, and so on, which causes a supercurrent. Andreev bound states can thus be used to explain the *Josephson supercurrent* microscopically.

The so-called Josephson effect is on the one hand the phenomenon of supercurrent through a

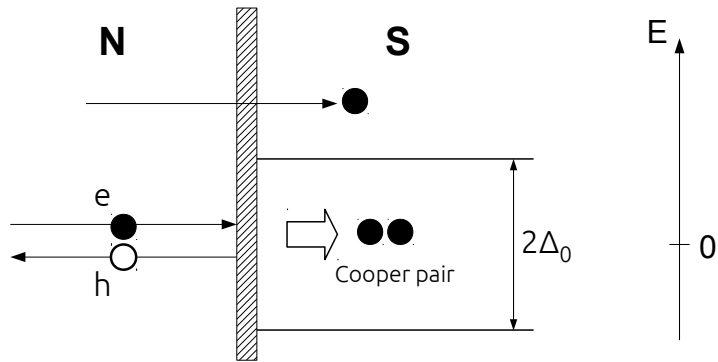


**Figure 2:** S-N junctions. There are different transport possibilities for electrons in a normal metal that is coupled to a superconductor. Electrons with energies larger than  $\Delta_0$  can tunnel into the superconductor. For energies smaller than  $\Delta_0$  electrons are either Andreev reflected or normal reflected.

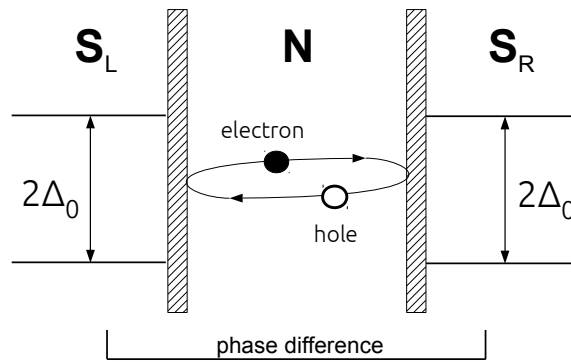


**Figure 3:** A normal metal confined between two superconductors. Andreev scattering can lead to bound states, if N is a nanostructure and there is a non-zero phase-difference between the superconductors.

device of two superconductors that are separated by a tunnel junction. The supercurrent occurs when there is a phase difference between the two superconductors, which can be produced by an external magnetic field. On the other hand, for a constant bias voltage the system also responds with an ac current, i.e., the phase difference changes with time.

### 3 Green functions

We study the transport of superconductor-dot junctions by means of Green functions. We are going to introduce the theory of Green functions based on the explanations in [7].

The Green function method is classically an important mathematical tool for solving inhomogeneous linear differential equations. This method has been adopted to solve different physical problems. Green functions are especially useful for systems treated by perturbation theory. To find, e.g., the solution to the time-dependent Schrödinger equation<sup>1</sup>

$$[i\partial_t - H_0(\mathbf{r}) - V(\mathbf{r})]\Psi(\mathbf{r}, t) = 0, \quad (3.1)$$

one defines the corresponding Green functions by the differential equations

$$[i\partial_t - H_0(\mathbf{r})]G_0(\mathbf{r}t, \mathbf{r}'t') = \delta(\mathbf{r} - \mathbf{r}')\delta(t - t'), \quad (3.2)$$

$$[i\partial_t - H_0(\mathbf{r}) - V(\mathbf{r})]G(\mathbf{r}t, \mathbf{r}'t') = \delta(\mathbf{r} - \mathbf{r}')\delta(t - t'), \quad (3.3)$$

and identifies the inverses of the Green functions as

$$G_0^{-1}(\mathbf{r}t, \mathbf{r}'t') = [i\partial_t - H_0(\mathbf{r})] \delta(\mathbf{r} - \mathbf{r}')\delta(t - t'), \quad (3.4)$$

$$G^{-1}(\mathbf{r}t, \mathbf{r}'t') = [i\partial_t - H_0(\mathbf{r}) - V(\mathbf{r})] \delta(\mathbf{r} - \mathbf{r}')\delta(t - t'). \quad (3.5)$$

The solution for the Schrödinger equation is found as

$$\Psi(\mathbf{r}, t) = \Psi^0(\mathbf{r}, t) + \int d\mathbf{r}' \int dt' G_0(\mathbf{r}t, \mathbf{r}'t') V(\mathbf{r}') \Psi(\mathbf{r}', t'), \quad (3.6)$$

$$\text{or } \Psi(\mathbf{r}, t) = \Psi^0(\mathbf{r}, t) + \int d\mathbf{r}' \int dt' G(\mathbf{r}t, \mathbf{r}'t') V(\mathbf{r}') \Psi^0(\mathbf{r}', t'), \quad (3.7)$$

where  $\Psi^0(\mathbf{r}, t)$  is the solution of the unperturbed Schrödinger equation. We can iterate the solution in Eq. (3.6),

$$\begin{aligned} \Psi &= \Psi^0 + G_0 V \Psi^0 + G_0 V G_0 V \Psi^0 + G_0 V G_0 V G_0 V \Psi^0 + \dots \\ &= \Psi^0 + (G_0 + G_0 V G_0 + G_0 V G_0 V G_0 + \dots) V \Psi^0, \end{aligned} \quad (3.8)$$

where we suppressed the integration variables for simplification. If we compare this with Eq. (3.7), we can identify the full Green function,

$$\begin{aligned} G &= G_0 + G_0 V G_0 + G_0 V G_0 V G_0 + \dots \\ &= G_0 + G_0 V (G_0 + G_0 V G_0 + \dots) \end{aligned} \quad (3.9)$$

The expression in parentheses can again be identified as  $G$ . Thus, we end up with the so-called Dyson equation,

$$G = G_0 + G_0 V G. \quad (3.10)$$

We can also write Eq. (3.9) as follows,

$$\begin{aligned} G &= G_0 + G_0 (V + V G_0 V + \dots) G_0 \\ &= G_0 + G_0 T G_0. \end{aligned} \quad (3.11)$$

---

<sup>1</sup>Note that we put  $\hbar = 1$  for any further calculations.

Here we defined the so-called  $T$ -matrix, which gives another possibility to determine the full Green function.

Green functions are often called propagators, because the wavefunction can be expressed in terms of the Green function as

$$\Psi(\mathbf{r}, t) = \int d\mathbf{r}' G(\mathbf{r}t, \mathbf{r}'t') \Psi(\mathbf{r}', t'), \quad (3.12)$$

i.e.,  $G(\mathbf{r}t, \mathbf{r}'t')$  propagates the wavefunction from an initial time  $t'$  to a time  $t$ .

### 3.1 Green functions for many-body systems

We are looking here in particular at the single-particle Green functions of many-body systems, which are expressed in second quantization. We will derive certain physical observables with the help of the Green functions, i.e., the spectral function or the current.

The Green functions are defined by a particle's initial and final space-time point  $\mathbf{r}'t'$  and  $\mathbf{r}t$ , as well as its initial and final spin  $\sigma'$  and  $\sigma$ . They give the probability for a particle to propagate from  $\mathbf{r}'t'$  to  $\mathbf{r}t$ .

The *time-ordered* Green function is of the most general form and is defined as

$$G_{\sigma\sigma'}^t(\mathbf{r}t, \mathbf{r}'t') = -i \langle T \Psi_{\sigma}(\mathbf{r}t) \Psi_{\sigma'}^{\dagger}(\mathbf{r}'t') \rangle, \quad (3.13)$$

where  $\langle \dots \rangle$  denotes the thermal average,  $T$  is the time-ordering operator and  $\Psi_{\sigma}(\mathbf{r}t)$  is the bosonic or fermionic field operator, which are second quantized objects.

We are working here in the Heisenberg picture, that means that the operators carry the time-dependence. An operator in the Heisenberg picture  $a(t)$  is defined via the operator in the Schrödinger picture  $a$ ,

$$a(t) = e^{iHt} a e^{-iHt}, \quad (3.14)$$

$$a^{\dagger}(t) = e^{iHt} a^{\dagger} e^{-iHt}, \quad (3.15)$$

where  $H$  is the system's full Hamiltonian.

The thermal average of a quantum operator  $A$  is

$$\langle A \rangle = \frac{1}{Z} \text{Tr}[\rho A], \quad (3.16)$$

where  $\text{Tr}[\dots]$  denotes the trace,  $\rho = e^{-\beta H}$  the density matrix and  $Z = \text{Tr}[\rho]$  is the partition function.

For two time-dependent operators  $A(t)$  and  $B(t')$  the time-ordering operator behaves as follows

$$T A(t) B(t') = \begin{cases} A(t) B(t'), & \text{if } t > t' \\ \pm B(t') A(t), & \text{if } t' > t, \end{cases} \quad (3.17)$$

where in the second line it is "+" or "-" depending whether the operators are bosonic or fermionic.

The quantum field operators are given by the single-particle basis set in the occupation number representation  $\{|\psi_{\nu}\rangle\} = \{|\nu\rangle\}$  as well as the creation and annihilation operators  $a_{\nu}^{\dagger}$  and  $a_{\nu}$ ,

$$\Psi^{\dagger}(\mathbf{r}t) \equiv \sum_{\nu} \langle \mathbf{r} | \psi_{\nu} \rangle^* a_{\nu}^{\dagger}(t) = \sum_{\nu} \psi_{\nu}^*(\mathbf{r}) a_{\nu}^{\dagger}(t), \quad \Psi(\mathbf{r}t) \equiv \sum_{\nu} \langle \mathbf{r} | \psi_{\nu} \rangle a_{\nu}(t) = \sum_{\nu} \psi_{\nu}(\mathbf{r}) a_{\nu}(t), \quad (3.18)$$

where  $\psi_\nu(\mathbf{r})$  is the ordinary first quantized wavefunction. The fundamental operators  $a_\nu$  and  $a_\nu^\dagger$  behave differently for bosons and fermions. We call the bosonic creation and annihilation operators  $b_\nu^\dagger$  and  $b_\nu$ . The time dependent operators obey the commutation relations

$$[b_{\nu_j}(t_1), b_{\nu_k}(t_2)] = 0, \quad [b_{\nu_j}^\dagger(t_1), b_{\nu_k}^\dagger(t_2)] = 0, \quad [b_{\nu_j}(t_1), b_{\nu_k}^\dagger(t_2)] = \delta_{\nu_j\nu_k} \delta(t_1 - t_2). \quad (3.19)$$

The time dependent fermionic creation and annihilation operators,  $c_\nu^\dagger(t)$  and  $c_\nu(t)$ , obey the anti-commutation relations

$$\{c_{\nu_j}(t_1), c_{\nu_k}(t_2)\} = 0, \quad \{c_{\nu_j}^\dagger(t_1), c_{\nu_k}^\dagger(t_2)\} = 0, \quad \{c_{\nu_j}(t_1), c_{\nu_k}^\dagger(t_2)\} = \delta_{\nu_j\nu_k} \delta(t_1 - t_2). \quad (3.20)$$

This leads to the (anti-)commutation relations for the field operators,

$$[\Psi(\mathbf{r}_1 t_1), \Psi(\mathbf{r}_2 t_2)]_{B,F} = 0, \quad (3.21)$$

$$[\Psi^\dagger(\mathbf{r}_1 t_1), \Psi^\dagger(\mathbf{r}_2 t_2)]_{B,F} = 0, \quad (3.22)$$

$$[\Psi(\mathbf{r}_1 t_1), \Psi^\dagger(\mathbf{r}_2 t_2)]_{B,F} = \delta(\mathbf{r}_1 - \mathbf{r}_2) \delta(t_1 - t_2), \quad (3.23)$$

where the (anti-)commutator  $[\dots, \dots]_{B,F}$  is defined as

$$[A, B]_B = [A, B] = AB - BA, \quad (3.24)$$

$$[A, B]_F = \{A, B\} = AB + BA. \quad (3.25)$$

There are more types of Green functions that are derived from the time-ordered one and that turned out to be particularly useful.

- The greater Green function

$$G_{\sigma\sigma'}^>(\mathbf{r}t, \mathbf{r}'t') = -i \langle \Psi_\sigma(\mathbf{r}t) \Psi_{\sigma'}^\dagger(\mathbf{r}'t') \rangle. \quad (3.26)$$

- The lesser Green function

$$G_{\sigma\sigma'}^<(\mathbf{r}t, \mathbf{r}'t') = -i(\pm) \langle \Psi_{\sigma'}^\dagger(\mathbf{r}'t') \Psi_\sigma(\mathbf{r}t) \rangle, \quad (3.27)$$

where it is "+" for bosons and "-" for fermions.

- The retarded Green function

$$G_{\sigma\sigma'}^R(\mathbf{r}t, \mathbf{r}'t') = -i\theta(t - t') \langle [\Psi_\sigma(\mathbf{r}t), \Psi_{\sigma'}^\dagger(\mathbf{r}'t')]_{B,F} \rangle, \quad (3.28)$$

collects all contributions that happen after  $t'$  and therefore describes how the presence of a particle at  $\mathbf{r}$  at time  $t$  depends on its position  $\mathbf{r}'$  at an earlier time  $t'$ .

- The advanced Green function

$$G_{\sigma\sigma'}^A(\mathbf{r}t, \mathbf{r}'t') = i\theta(t' - t) \langle [\Psi_\sigma(\mathbf{r}t), \Psi_{\sigma'}^\dagger(\mathbf{r}'t')]_{B,F} \rangle, \quad (3.29)$$

collects all contributions that happened before  $t'$  and therefore describes how the presence of a particle at  $\mathbf{r}$  at time  $t$  depends on its position  $\mathbf{r}'$  at a future time  $t'$ .

The retarded and advanced Green functions are related to the lesser and greater Green functions via

$$G_{\sigma\sigma'}^R(\mathbf{r}t, \mathbf{r}'t') = \theta(t - t')[G_{\sigma\sigma'}^>(\mathbf{r}t, \mathbf{r}'t') - G_{\sigma\sigma'}^<(\mathbf{r}t, \mathbf{r}'t')], \quad (3.30)$$

$$G_{\sigma\sigma'}^A(\mathbf{r}t, \mathbf{r}'t') = \theta(t' - t)[G_{\sigma\sigma'}^<(\mathbf{r}t, \mathbf{r}'t') - G_{\sigma\sigma'}^>(\mathbf{r}t, \mathbf{r}'t')]. \quad (3.31)$$

This further gives

$$G_{\sigma\sigma'}^R(\mathbf{r}t, \mathbf{r}'t') - G_{\sigma\sigma'}^A(\mathbf{r}t, \mathbf{r}'t') = G_{\sigma\sigma'}^>(\mathbf{r}t, \mathbf{r}'t') - G_{\sigma\sigma'}^<(\mathbf{r}t, \mathbf{r}'t'). \quad (3.32)$$

The following useful relations can be obtained from the definition of the corresponding Green functions,

$$G_{\sigma\sigma'}^R(\mathbf{r}t, \mathbf{r}'t')^* = G_{\sigma'\sigma}^A(\mathbf{r}'t', \mathbf{r}t), \quad (3.33)$$

$$G_{\sigma\sigma'}^<(\mathbf{r}t, \mathbf{r}'t')^* = -G_{\sigma'\sigma}^<(\mathbf{r}'t', \mathbf{r}t). \quad (3.34)$$

We can also write Green functions in a general  $|\nu\rangle$ -basis, where  $\nu$  stands for all the relevant quantum numbers,

$$G_{\nu\sigma, \nu'\sigma'}^t(t, t') = -i\langle T a_{\nu\sigma}(t) a_{\nu'\sigma'}^\dagger(t') \rangle, \quad (3.35)$$

which is related to the real space time-ordered Green function via

$$G_{\sigma\sigma'}^t(\mathbf{r}t, \mathbf{r}'t') = \sum_{\nu\nu'} \psi_{\nu\sigma}(\mathbf{r}) G_{\nu\sigma, \nu'\sigma'}^t(t, t') \psi_{\nu'\sigma'}^*(\mathbf{r}'). \quad (3.36)$$

The notation in Eq. (3.35) is more convenient and therefore used more often. We can of course write the greater, lesser, retarded and advanced Green functions in this basis as well,

$$G_{\nu\sigma, \nu'\sigma'}^>(t, t') = -i\langle a_{\nu\sigma}(t) a_{\nu'\sigma'}^\dagger(t') \rangle, \quad (3.37)$$

$$G_{\nu\sigma, \nu'\sigma'}^<(t, t') = -i(\pm)\langle a_{\nu'\sigma'}^\dagger(t') a_{\nu\sigma}(t) \rangle, \quad (3.38)$$

$$G_{\nu\sigma, \nu'\sigma'}^R(t, t') = -i\theta(t - t')\langle [a_{\nu\sigma}(t), a_{\nu'\sigma'}^\dagger(t')]_{B,F} \rangle, \quad (3.39)$$

$$G_{\nu\sigma, \nu'\sigma'}^A(t, t') = i\theta(t' - t)\langle [a_{\nu\sigma}(t), a_{\nu'\sigma'}^\dagger(t')]_{B,F} \rangle. \quad (3.40)$$

## 3.2 Equation of motion theory

When we are going to derive the spectral function or the current, we will have to calculate the time dependence of the Green functions. One way of doing that would be to use the equation of motion technique. The idea is here, that one differentiates the definition of the Green function with respect to the time. Then one uses the Heisenberg equation of motion to calculate the time derivative of the operators. Then one obtains a differential equation, which one has to solve.

The idea is to differentiate the Green function a couple of times to get a closed set of equations that solve the problem.

Let us for example consider the time-ordered Green function in a general  $|\nu\rangle$ -basis,

$$G_{\nu\sigma, \nu'\sigma'}^t(t, t') = -i\langle T a_{\nu\sigma}(t) a_{\nu'\sigma'}^\dagger(t') \rangle \quad (3.41)$$

$$= -i \left[ \theta(t - t') \langle a_{\nu\sigma}(t) a_{\nu'\sigma'}^\dagger(t') \rangle \pm \theta(t' - t) \langle a_{\nu'\sigma'}^\dagger(t') a_{\nu\sigma}(t) \rangle \right]. \quad (3.42)$$

Here we rewrote the time-ordering operator  $T$  in terms of the step function. Then the differentiation with respect to  $t$  gives

$$\partial_t G_{\nu\sigma,\nu'\sigma'}^t(t,t') = -i\delta(t-t')\langle [a_{\nu\sigma}(t), a_{\nu'\sigma'}^\dagger(t')]_{B,F} \rangle - i\langle T \partial_t a_{\nu\sigma}(t) a_{\nu'\sigma'}^\dagger(t') \rangle \quad (3.43)$$

$$= -i\delta_{\nu\nu'}\delta_{\sigma\sigma'}\delta(t-t') + \langle T [H, a_{\nu\sigma}(t)] a_{\nu'\sigma'}^\dagger(t') \rangle, \quad (3.44)$$

where we used the fact, that the time derivative of the step function gives the delta function. Furthermore, we used that the time derivative of an operator in the Heisenberg picture is given by the commutator with the Hamiltonian,  $\partial_t a_{\nu\sigma}(t) = i[H, a_{\nu\sigma}(t)]$ . The next step would be to calculate the commutator. Then we might be able to identify further Green functions in the equation.

In the next section we will see, that the Green functions only depend on the time difference  $t - t'$ . This is because the Hamiltonian does not depend explicitly on time. Therefore, it will be useful to work with the Fourier transforms of the Green functions.

### 3.3 The Lehmann representation

We are now going to write the Green functions in the Lehmann representation, i.e, we use the set of eigenstates,  $\{|n\rangle\}$ , of the full Hamiltonian,  $H$ , as a basis set to spectrally decompose the Green functions. We will be able to express the Fourier transformed lesser or greater Green function in terms of the spectral function.

From now on we look at fermionic Green functions. Calculations for bosons go equivalently.

#### 3.3.1 Lesser and greater Green function

First, let us have a look at the lesser Green function in the  $|\nu\rangle$ -basis,

$$G_{\nu\nu'}^<(t,t') = i\langle c_{\nu'}^\dagger(t')c_\nu(t) \rangle. \quad (3.45)$$

The fermion creation and annihilation operators are given in the Heisenberg picture,

$$c_\nu^\dagger(t) = e^{iHt}c_\nu^\dagger e^{-iHt}, \quad (3.46)$$

$$c_\nu(t) = e^{iHt}c_\nu e^{-iHt}. \quad (3.47)$$

We now insert  $1 = \sum_n |n\rangle\langle n|$  into Eq. (3.45) and use the thermal average of an operator (3.16),

$$G_{\nu\nu'}^<(t,t') = \frac{i}{Z} \sum_{nn'} e^{-\beta E_n} \langle n|c_{\nu'}^\dagger(t')|n'\rangle \langle n'|c_\nu(t)|n\rangle \quad (3.48)$$

$$= \frac{i}{Z} \sum_{nn'} e^{-\beta E_n} \langle n|c_{\nu'}^\dagger|n'\rangle \langle n'|c_\nu|n\rangle e^{i(E_{n'}-E_n)(t-t')} \quad (3.49)$$

$$= G_{\nu\nu'}^<(t-t'), \quad (3.50)$$

where the partition function  $Z = \text{Tr}[\rho] = \sum_n \langle n|e^{-\beta H}|n\rangle$  is a real number. We see that the Green function does only depend on the time difference  $t - t'$ . Shifting the time argument  $t - t' \rightarrow t$  and Fourier transforming this equation gives

$$G_{\nu\nu'}^<(\omega) = \frac{2\pi i}{Z} \sum_{nn'} e^{-\beta E_n} \langle n|c_{\nu'}^\dagger|n'\rangle \langle n'|c_\nu|n\rangle \delta(E_{n'} - E_n + \omega). \quad (3.51)$$

Here we used that the Fourier transformation of  $e^{i\omega t}$  gives

$$\int_{-\infty}^{\infty} dt e^{i\omega t} = 2\pi\delta(\omega). \quad (3.52)$$

We do the same for the greater Green function,

$$G_{\nu\nu'}^>(t, t') = -i\langle c_\nu(t)c_{\nu'}^\dagger(t') \rangle \quad (3.53)$$

$$= -\frac{i}{Z} \sum_{nn'} e^{-\beta E_n} \langle n|c_\nu|n' \rangle \langle n'|c_{\nu'}^\dagger|n \rangle e^{i(E_n - E_{n'})(t-t')} \quad (3.54)$$

$$= G_{\nu\nu'}^>(t - t'). \quad (3.55)$$

Using again Eq. (3.52) we obtain in the frequency domain

$$G_{\nu\nu'}^>(\omega) = -\frac{2\pi i}{Z} \sum_{nn'} e^{-\beta E_n} \langle n|c_\nu|n' \rangle \langle n'|c_{\nu'}^\dagger|n \rangle \delta(E_n - E_{n'} + \omega) \quad (3.56)$$

$$= -\frac{2\pi i}{Z} \sum_{nn'} e^{-\beta E_{n'}} \langle n'|c_\nu|n \rangle \langle n|c_{\nu'}^\dagger|n' \rangle \delta(E_{n'} - E_n + \omega) \quad (3.57)$$

$$= -\frac{2\pi i}{Z} \sum_{nn'} e^{-\beta(E_n - \omega)} \langle n|c_{\nu'}^\dagger|n' \rangle \langle n'|c_\nu|n \rangle \delta(E_{n'} - E_n + \omega), \quad (3.58)$$

where we used the fact that, because of the delta function, this equation is only non-zero where  $E_{n'} = E_n - \omega$ . Thus, we found the following relation between lesser and greater Green function,

$$G_{\nu\nu'}^>(\omega) = -e^{\beta\omega} G_{\nu\nu'}^<(\omega). \quad (3.59)$$

### 3.3.2 Retarded and advanced Green function

In the Lehmann representation the retarded Green function turns to

$$G_{\nu\nu'}^R(t, t') = -i\theta(t - t') \langle \{c_\nu(t), c_{\nu'}^\dagger(t')\} \rangle \quad (3.60)$$

$$= -i\theta(t - t') \langle c_\nu(t)c_{\nu'}^\dagger(t') \rangle - i\theta(t - t') \langle c_{\nu'}^\dagger(t')c_\nu(t) \rangle \quad (3.61)$$

$$= -i\theta(t - t') \frac{1}{Z} \sum_{nn'} e^{-\beta E_n} \left( \langle n|c_\nu|n' \rangle \langle n'|c_{\nu'}^\dagger|n \rangle e^{i(E_n - E_{n'})(t-t')} \right. \\ \left. + \langle n|c_{\nu'}^\dagger|n' \rangle \langle n'|c_\nu|n \rangle e^{-i(E_n - E_{n'})(t-t')} \right) \quad (3.62)$$

$$= G_{\nu\nu'}^R(t - t'). \quad (3.63)$$

When Fourier transforming the retarded Green function we set again  $t - t' \rightarrow t$ . Because of the step function, we get an integral of the form  $\int_0^\infty dt e^{i\omega t}$ , i.e., we cannot use the relation from Eq. (3.52) here. To ensure that the integrand decays for  $t \rightarrow \infty$  we subtract  $\eta t$  from  $i\omega t$ , where  $\eta \rightarrow 0^+$  is a positive infinitesimal. This corresponds to making the frequency complex,  $\omega \rightarrow \omega + i\eta$ .

For the Fourier transformation of the advanced Green function we have to put  $\omega \rightarrow \omega - i\eta$ , since there we have the integration limit  $t \rightarrow -\infty$ .

Thus, we are able to perform the integral, as the following relation holds for  $\eta > 0$ ,

$$\int_{-\infty}^{\infty} dt \theta(\pm t) e^{i(\omega \pm i\eta)t} = \frac{\pm i}{\omega \pm i\eta}. \quad (3.64)$$

Hence, the Fourier transformation of the retarded Green function is

$$G_{\nu\nu'}^R(\omega) = -i \int_{-\infty}^{\infty} dt \theta(t) e^{i(\omega+i\eta)t} \frac{1}{Z} \sum_{nn'} e^{-\beta E_n} \left( \langle n|c_\nu|n'\rangle \langle n'|c_{\nu'}^\dagger|n\rangle e^{i(E_n-E_{n'})t} + \langle n|c_{\nu'}^\dagger|n'\rangle \langle n'|c_\nu|n\rangle e^{-i(E_n-E_{n'})t} \right) \quad (3.65)$$

$$= \frac{1}{Z} \sum_{nn'} e^{-\beta E_n} \left( \frac{\langle n|c_\nu|n'\rangle \langle n'|c_{\nu'}^\dagger|n\rangle}{\omega + E_n - E_{n'} + i\eta} + \frac{\langle n|c_{\nu'}^\dagger|n'\rangle \langle n'|c_\nu|n\rangle}{\omega - E_n + E_{n'} + i\eta} \right) \quad (3.66)$$

$$= \frac{1}{Z} \sum_{nn'} \frac{\langle n|c_\nu|n'\rangle \langle n'|c_{\nu'}^\dagger|n\rangle}{\omega + E_n - E_{n'} + i\eta} (e^{-\beta E_n} + e^{-\beta E_{n'}}). \quad (3.67)$$

The same procedure holds for the advanced Green function,

$$G_{\nu\nu'}^A(t, t') = i\theta(t' - t) \langle \{c_\nu(t), c_{\nu'}^\dagger(t')\} \rangle. \quad (3.68)$$

We do the same steps as before, i.e., write explicitly the thermal average and the Heisenberg representation of the operators. For the Fourier transformation we put  $\omega \rightarrow \omega - i\eta$ , then we use the relation Eq. (3.64) to perform the integral. This results in

$$G_{\nu\nu'}^A(\omega) = \frac{1}{Z} \sum_{nn'} \frac{\langle n|c_\nu|n'\rangle \langle n'|c_{\nu'}^\dagger|n\rangle}{\omega + E_n - E_{n'} - i\eta} (e^{-\beta E_n} + e^{-\beta E_{n'}}). \quad (3.69)$$

As we see the retarded and advanced Green functions only differ in the sign in front of the positive infinitesimal. We can find a relation between the advanced and retarded Green function here, too.

We complex conjugate  $G_{\nu\nu'}^A(\omega)$  and compare it to the retarded Green function,

$$G_{\nu\nu'}^{A*}(\omega) = \frac{1}{Z} \sum_{nn'} \frac{\langle n'|c_{\nu'}^\dagger|n\rangle \langle n|c_\nu|n'\rangle}{\omega + E_n - E_{n'} + i\eta} (e^{-\beta E_n} + e^{-\beta E_{n'}}) \quad (3.70)$$

$$= G_{\nu'\nu}^R(\omega). \quad (3.71)$$

### 3.3.3 Spectral function

We now want to treat the spectral function. In the Lehmann representation, it reveals further relations between the different types of Green functions.

The spectral function gives the energy resolution for a given quantum state. It is defined as

$$A_{\nu\nu'}(\omega) = i[G_{\nu\nu'}^R(\omega) - G_{\nu\nu'}^A(\omega)]. \quad (3.72)$$

It indicates the distribution of excitations, when a particle with certain quantum numbers  $\nu, \nu'$  is added to a given system. For normal metals, the spectral function is usually diagonal  $A_{\nu\nu'} = \delta_{\nu\nu'} A_\nu$ , because an electron can only be in either  $|\nu\rangle$  or  $|\nu'\rangle$ . When we treat superconductors, we have pairs of electrons, which are of different quantum states. Recall, a Cooper pair consists of a pair of electrons with the states  $|\mathbf{k} \uparrow\rangle$  and  $|\mathbf{k} \downarrow\rangle$ . This will give as well off-diagonal terms for the spectral function.

As we will see later, the spectral function for a system of non-interacting free particles is proportional to the delta function  $\delta(\omega - \xi_\nu)$ . This means, that there can only be an excitation with energy  $\omega$ , when a particle with energy  $\xi_\nu$  is added, as we would have expected.

For systems with interacting particles, the spectral function broadens. Remember, that in a superconductor we have electron-electron as well as electron-phonon interaction, which means energy

exchange. Conclusively, the spectrum for the superconductor should broaden. As we only do mean-field theory here, we will not encounter a broadened spectrum, except for  $\eta$ , which can be interpreted as an artificial broadening.

Let us now have a closer look at the definition of the spectral function, Eq. (3.72). The difference between retarded and advanced Green function in Lehmann representation is from what we found in Eq. (3.67) and Eq. (3.69),

$$G_{\nu\nu'}^R(\omega) - G_{\nu\nu'}^A(\omega) = \frac{1}{Z} \sum_{nn'} \langle n|c_\nu|n'\rangle \langle n'|c_{\nu'}^\dagger|n\rangle (e^{-\beta E_n} + e^{-\beta E_{n'}}) \times \left( \frac{1}{\omega + E_n - E_{n'} + i\eta} - \frac{1}{\omega + E_n - E_{n'} - i\eta} \right). \quad (3.73)$$

To further simplify this expression, we benefit from the following relation,

$$\frac{1}{x \pm i\eta} = \mathcal{P} \left( \frac{1}{x} \right) \mp i\pi\delta(x), \quad (3.74)$$

where  $\mathcal{P}$  denotes the principal value and for our case it is  $x = \omega + E_n - E_{n'}$ . This is also known by the name *Sokhotski–Plemelj theorem* and is valid, if  $\eta$  is a positive infinitesimal. The expression in parentheses in Eq. (3.73) then simplifies to

$$\frac{1}{\omega + E_n - E_{n'} + i\eta} - \frac{1}{\omega + E_n - E_{n'} - i\eta} = -2\pi i\delta(\omega + E_n - E_{n'}). \quad (3.75)$$

If we plug this back into Eq. (3.73), we get

$$G_{\nu\nu'}^R(\omega) - G_{\nu\nu'}^A(\omega) = \frac{-2\pi i}{Z} \sum_{nn'} \langle n|c_\nu|n'\rangle \langle n'|c_{\nu'}^\dagger|n\rangle (e^{-\beta E_n} + e^{-\beta E_{n'}}) \delta(\omega + E_n - E_{n'}). \quad (3.76)$$

If we compare this to the the lesser and greater Green functions, Eqs. (3.51) and (3.56), we see that this gives the equality

$$G_{\nu\nu'}^R(\omega) - G_{\nu\nu'}^A(\omega) = G_{\nu\nu'}^>(\omega) - G_{\nu\nu'}^<(\omega) \quad (3.77)$$

$$= -(1 + e^{\beta\omega})G_{\nu\nu'}^<(\omega), \quad (3.78)$$

where we used the relation between lesser and greater Green function Eq. (3.59). Here, we can identify the Fermi distribution  $n_F(\omega) = (1 + e^{\beta\omega})^{-1}$ . We further rewrite this by means of the spectral function, Eq. (3.72). We end up with an expression for the lesser Green function in terms of the Fermi function and the spectral function,

$$G_{\nu\nu'}^<(\omega) = in_F(\omega)A_{\nu\nu'}(\omega). \quad (3.79)$$

Of course, there is also a similar expression for the greater Green function,

$$G_{\nu\nu'}^>(\omega) = -i[1 - n_F(\omega)]A_{\nu\nu'}(\omega). \quad (3.80)$$

These relations for the lesser and greater Green functions are also known as the *fluctuation-dissipation theorem*.

### 3.4 Imaginary-time Green functions

Replacing the time argument by an imaginary quantity  $t \rightarrow -i\tau$ , where  $\tau$  is real and of time dimension, is a mathematical method to work out the retarded Green function. The imaginary-time Green function is also known by the name Matsubara Green function. The single particle Matsubara Green function for either bosons or fermions is defined as follows,

$$\mathcal{G}_{\nu\nu'}(\tau, \tau') \equiv -\langle T_\tau a_\nu(\tau) a_{\nu'}^\dagger(\tau') \rangle. \quad (3.81)$$

Here we introduced the time-ordering operator in imaginary time,

$$T_\tau A(\tau)B(\tau') = \theta(\tau - \tau')A(\tau)B(\tau') \pm \theta(\tau' - \tau)B(\tau')A(\tau), \quad (3.82)$$

where it is "+" for bosons or "-" for fermions. We also defined the imaginary-time Heisenberg picture by substituting  $it$  by  $\tau$ . Therefore, an operator in the Heisenberg picture is defined via an operator  $A$  in the Schrödinger picture as

$$A(\tau) = e^{\tau H} A e^{-\tau H}, \quad (3.83)$$

where  $H$  is the time-independent Hamiltonian.

It can be shown by means of the thermal average, that the Matsubara Green function depends only on the time difference, since for  $\tau > \tau'$ ,

$$\begin{aligned} \mathcal{G}_{\nu\nu'}(\tau, \tau') &= -\frac{1}{Z} \text{Tr} \left[ e^{-\beta H} e^{\tau H} a_\nu e^{-\tau H} e^{\tau' H} a_{\nu'}^\dagger e^{-\tau' H} \right] \\ &= -\frac{1}{Z} \text{Tr} \left[ e^{-\beta H} e^{-\tau' H} e^{\tau H} a_\nu e^{-\tau H} e^{\tau' H} a_{\nu'}^\dagger \right] \\ &= -\frac{1}{Z} \text{Tr} \left[ e^{-\beta H} e^{(\tau-\tau')H} a_\nu e^{-(\tau-\tau')H} a_{\nu'}^\dagger \right] \\ &= \mathcal{G}_{\nu\nu'}(\tau - \tau'), \end{aligned} \quad (3.84)$$

where we used the cyclic property of the trace. For the case  $\tau < \tau'$  it is  $\mathcal{G}_{\nu\nu'}(\tau, \tau') = \mathcal{G}_{\nu\nu'}(\tau' - \tau)$ . Therefore, the Matsubara Green function in Eq. (3.81) can be written as well as

$$\mathcal{G}_{\nu\nu'}(\tau) = -\langle T_\tau a_\nu(\tau) a_{\nu'}^\dagger(0) \rangle. \quad (3.85)$$

If we use the Lehmann representation of Eq. (3.84), we find that the time argument is constrained to  $-\beta < \tau - \tau' < \beta$ . This is to guarantee convergence of the Green function.

From the cyclic property of the trace, we further find the symmetry properties of the Matsubara Green function,

$$\mathcal{G}_{\nu\nu'}(\tau) = \pm \begin{cases} \mathcal{G}_{\nu\nu'}(\tau + \beta) & \text{for } -\beta < \tau < 0, \\ \mathcal{G}_{\nu\nu'}(\tau - \beta) & \text{for } 0 < \tau < \beta, \end{cases} \quad (3.86)$$

where it is "+" for bosons and "-" for fermions.

#### 3.4.1 Fourier transform of Matsubara Green functions

We would like to Fourier transform the Matsubara Green function with respect to the imaginary time. Since we got the Matsubara Green function  $\mathcal{G}_{\nu\nu'}(\tau)$  defined in the interval  $-\beta < \tau < \beta$ , it can

be expanded in a Fourier series,

$$\mathcal{G}_{\nu\nu'}(\tau) = \frac{1}{\beta} \sum_{\tilde{\omega}_n} e^{-i\tilde{\omega}_n\tau} \mathcal{G}_{\nu\nu'}(i\tilde{\omega}_n), \quad (3.87)$$

$$\mathcal{G}_{\nu\nu'}(i\tilde{\omega}_n) = \frac{1}{2} \int_{-\beta}^{\beta} d\tau e^{i\tilde{\omega}_n\tau} \mathcal{G}_{\nu\nu'}(\tau), \quad (3.88)$$

with the frequencies<sup>2</sup>  $\tilde{\omega}_n = 2\pi n/2\beta = \pi n/\beta$ , where  $n \in \mathbb{Z}$ . Using the symmetry property (3.86) we can rewrite Eq. (3.88),

$$\mathcal{G}_{\nu\nu'}(i\tilde{\omega}_n) = \frac{1}{2} \int_{-\beta}^0 d\tau e^{i\tilde{\omega}_n\tau} \mathcal{G}_{\nu\nu'}(\tau) + \frac{1}{2} \int_0^{\beta} d\tau e^{i\tilde{\omega}_n\tau} \mathcal{G}_{\nu\nu'}(\tau) \quad (3.89)$$

$$= \frac{1}{2} \int_0^{\beta} d\tau e^{i\tilde{\omega}_n(\tau-\beta)} \mathcal{G}_{\nu\nu'}(\tau - \beta) + \frac{1}{2} \int_0^{\beta} d\tau e^{i\tilde{\omega}_n\tau} \mathcal{G}_{\nu\nu'}(\tau) \quad (3.90)$$

$$= \frac{1}{2} (1 \pm e^{-i\pi n}) \int_0^{\beta} d\tau e^{i\tilde{\omega}_n\tau} \mathcal{G}_{\nu\nu'}(\tau). \quad (3.91)$$

The prefactor of Eq. (3.91) depends on whether we are looking at bosons or fermions as well as on the integer  $n$ . For the different types of particles it depends on whether  $n$  is an even or odd number,

$$\text{bosons : } \frac{1}{2} (1 + e^{-i\pi n}) = \begin{cases} 1, & n \text{ even} \\ 0, & n \text{ odd,} \end{cases} \quad \text{fermions : } \frac{1}{2} (1 - e^{-i\pi n}) = \begin{cases} 1, & n \text{ odd} \\ 0, & n \text{ even.} \end{cases} \quad (3.92)$$

Hence, we can write the Fourier transformation of the Matsubara Green function by means of the Matsubara frequency  $\omega_n$  with  $n \in \mathbb{Z}$  as follows,

$$\mathcal{G}_{\nu\nu'}(i\omega_n) = \int_0^{\beta} d\tau e^{i\omega_n\tau} \mathcal{G}_{\nu\nu'}(\tau), \quad \begin{cases} \omega_n = \frac{2n\pi}{\beta}, & \text{for bosons} \\ \omega_n = \frac{(2n+1)\pi}{\beta}, & \text{for fermions.} \end{cases} \quad (3.93)$$

### 3.4.2 Equation of motion for Matsubara Green functions

The equation of motion technique goes slightly different here, since we replaced the time argument  $t$  by the imaginary time  $-i\tau$  when we introduced the Matsubara Green function. We differentiate here the Matsubara Green function in Eq. (3.85) with respect to  $\tau$ , which gives

$$\begin{aligned} \partial_{\tau} \mathcal{G}_{\nu\nu'}(\tau) &= -\delta(\tau) \langle [a_{\nu}(\tau), a_{\nu'}^{\dagger}(0)]_{B,F} \rangle - \langle T_{\tau} \partial_{\tau} a_{\nu}(\tau) a_{\nu'}^{\dagger}(0) \rangle \\ &= -\delta_{\nu\nu'} \delta(\tau) - \langle T_{\tau} [H, a_{\nu}](\tau) a_{\nu'}^{\dagger}(0) \rangle. \end{aligned} \quad (3.94)$$

Here we used, that in the imaginary time formalism the time derivative of an operator in the Heisenberg picture is

$$\begin{aligned} \partial_{\tau} A(\tau) &= \partial_{\tau} (e^{\tau H} A e^{-\tau H}) \\ &= H e^{\tau H} A e^{-\tau H} - e^{\tau H} A H e^{-\tau H} \\ &= e^{\tau H} [H, A] e^{-\tau H} \\ &= [H, A](\tau). \end{aligned} \quad (3.95)$$

Note that the Hamiltonian  $H$  commutes with  $e^{\tau H}$ .

<sup>2</sup>Note that we denoted the frequency here with a tilde, since we will define a slightly different frequency in a moment, which we want to call  $\omega_n$ .

### 3.4.3 Connection between Matsubara and retarded Green function

We would like to show how the retarded Green function can be obtained from the Matsubara Green function, which is also why we introduced the Matsubara Green function in the first place. We can again use the Lehmann representation to rewrite the Matsubara Green function in Eq. (3.85). For  $\tau > 0$  it is,

$$\mathcal{G}_{\nu\nu'}(\tau) = -\langle a_\nu(\tau)a_{\nu'}^\dagger(0) \rangle \quad (3.96)$$

$$= -\frac{1}{Z} \sum_{nn'} e^{-\beta E_n} \langle n|a_\nu|n'\rangle \langle n'|a_{\nu'}^\dagger|n\rangle e^{\tau(E_n - E_{n'})}. \quad (3.97)$$

The Fourier transformation of this gives according to Eq. (3.93),

$$\mathcal{G}_{\nu\nu'}(i\omega_l) = \frac{1}{Z} \sum_{nn'} \frac{\langle n|a_\nu|n'\rangle \langle n'|a_{\nu'}^\dagger|n\rangle}{i\omega_l + E_n - E_{n'}} [e^{-\beta E_n} - (\pm)e^{-\beta E_{n'}}]. \quad (3.98)$$

Here, we wrote the Matsubara frequency with index  $l \in \mathbb{Z}$  to not to get confused with the eigenstates. The " $\pm$ " is again for either bosons or fermions. If we look at the Fourier transform of the retarded Green function in Lehmann representation, Eq. (3.67), but now general for bosons or fermions, we have a similar expression,

$$G_{\nu\nu'}^R(\omega) = \frac{1}{Z} \sum_{nn'} \frac{\langle n|a_\nu|n'\rangle \langle n'|a_{\nu'}^\dagger|n\rangle}{\omega + E_n - E_{n'} + i\eta} (e^{-\beta E_n} - (\pm)e^{-\beta E_{n'}}). \quad (3.99)$$

We find, that we can obtain the retarded Green function by doing the analytic continuation of the Matsubara Green function on the upper half of the complex plane and then approaching the real axis,  $i\omega_l \rightarrow z \rightarrow \omega + i\eta$ . To get the advanced Green function we do the continuation on the lower half plane,  $i\omega_l \rightarrow z \rightarrow \omega - i\eta$ . Thus, in short notation, the retarded and advanced Green function are obtain from the Matsubara Green function via

$$G_{\nu\nu'}^R(\omega) = \mathcal{G}_{\nu\nu'}(i\omega_l \rightarrow \omega + i\eta), \quad (3.100)$$

$$G_{\nu\nu'}^A(\omega) = \mathcal{G}_{\nu\nu'}(i\omega_l \rightarrow \omega - i\eta). \quad (3.101)$$

## 3.5 Contour ordered Green functions

If one does perturbation theory for Green functions, one encounters the contour ordered Green functions [10, 11]. They are defined as follows, where the time arguments of the contour are called  $\tau, \tau'$  here,

$$G_{\nu\nu'}^C(\tau, \tau') = -i\langle T_C c_\nu(\tau)c_{\nu'}^\dagger(\tau') \rangle. \quad (3.102)$$

The contour  $C$  runs infinitely close to the real time axis. It starts and ends at some initial time  $t_0$ , that one often puts to  $t_0 \rightarrow -\infty$ . It thus consists of two parts, where the first one is from  $-\infty$  to  $\infty$  and the second one runs from  $\infty$  to  $-\infty$ .  $T_C$  is the contour ordering operator, i.e., operators with time arguments that come later on the contour stand left from operators with times that come earlier. Consider now the following contour integral,

$$G_1^C(\tau, \tau') = \int_C d\tau_1 G_2^C(\tau, \tau_1) G_3^C(\tau_1, \tau'), \quad (3.103)$$

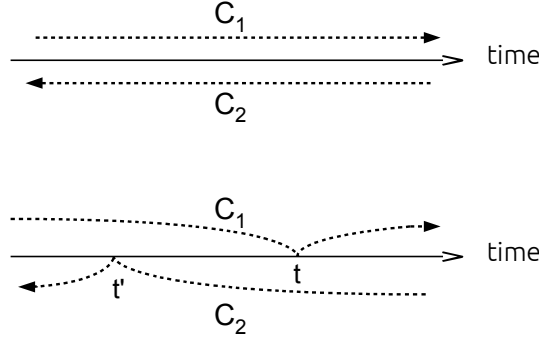


**Figure 4:** The contour ordered Green function is defined on  $C = C_1 + C_2$ , where  $C_1$  goes from  $-\infty$  to  $+\infty$  and  $C_2$  from  $+\infty$  to  $-\infty$ . Lower picture: to obtain the lesser Green function one deforms the contour so that the usually later time comes before the earlier time.

where the integration runs over the contour  $\int_C = \int_{C_1} + \int_{C_2}$ , where  $C_1$  goes from  $-\infty$  to  $\infty$  and  $C_2$  from  $\infty$  back to  $-\infty$ . It is also shown in Fig. 4. Those contour integrals occur for nonequilibrium Green functions.

If we are interested in  $G_1^<(t, t')$ , we deform the contour in Eq. (3.103), so that  $t$  lies on  $C_1$  and  $t'$  on  $C_2$ , Fig. 4. Therefore,  $t'$  is a later time than  $t$  on the contour, even though it might be  $t' < t$ . Thus, the contour ordered Green function turns into the lesser Green function.

Let us have a look at the first part of the integral of  $G_1^<(t, t')$ ,

$$\int_{C_1} d\tau_1 G_2^{C_1}(t, \tau_1) G_3^{C_1}(\tau_1, t') = \int_{-\infty}^{\infty} d\tau_1 G_2^t(t, \tau_1) G_3^<(\tau_1, t'). \quad (3.104)$$

Since  $\tau_1$  and  $t$  are both times that occur on  $C_1$ , the first Green function turns into the normal time ordered Green function. Since  $t'$  is a time of  $C_2$ ,  $\tau_1$  is always earlier, whereby the other function turns into the lesser Green function. Same principles for the second half of the contour integral gives

$$\int_{C_2} d\tau_1 G_2^{C_2}(t, \tau_1) G_3^{C_2}(\tau_1, t') = \int_{\infty}^{-\infty} d\tau_1 G_2^<(t, \tau_1) G_3^{\tilde{t}}(\tau_1, t'). \quad (3.105)$$

Since we go backwards in time, we obtain the anti-time ordered Green function  $G_3^{\tilde{t}}(\tau_1, t')$  here, which is defined through the anti-time-ordering operator  $\tilde{T}$ , i.e., operators with later time arguments go right from those with earlier times.

We now use some relations, that one can find directly from the definitions of the Green functions, Eq. (3.35) - (3.40),

$$G^t(t, \tau_1) = G^R(t, \tau_1) + G^<(t, \tau_1), \quad (3.106)$$

$$G^{\tilde{t}}(\tau_1, t') = G^<(\tau_1, t') - G^A(\tau_1, t'). \quad (3.107)$$

If we use these relations for the  $C_1$ - and  $C_2$ -integral of Eq. (3.103), we obtain the following expression for the lesser Green function,

$$G_1^<(t, t') = \int_{-\infty}^{\infty} d\tau_1 [G_2^R(t, \tau_1) G_3^<(\tau_1, t') + G_2^<(t, \tau_1) G_3^A(\tau_1, t')]. \quad (3.108)$$

This is one of the so-called *Langreth rules*. We can derive the relations for the other Green functions from Eq. (3.103) as well. We just have to deform the contour accordingly. The other Langreth rules are then,

$$G_1^>(t, t') = \int_{-\infty}^{\infty} d\tau_1 [G_2^R(t, \tau_1)G_3^>(\tau_1, t') + G_2^>(t, \tau_1)G_3^A(\tau_1, t')], \quad (3.109)$$

$$G_1^R(t, t') = \int_{-\infty}^{\infty} d\tau_1 G_2^R(t, \tau_1)G_3^R(\tau_1, t'), \quad (3.110)$$

$$G_1^A(t, t') = \int_{-\infty}^{\infty} d\tau_1 G_2^A(t, \tau_1)G_3^A(\tau_1, t'). \quad (3.111)$$

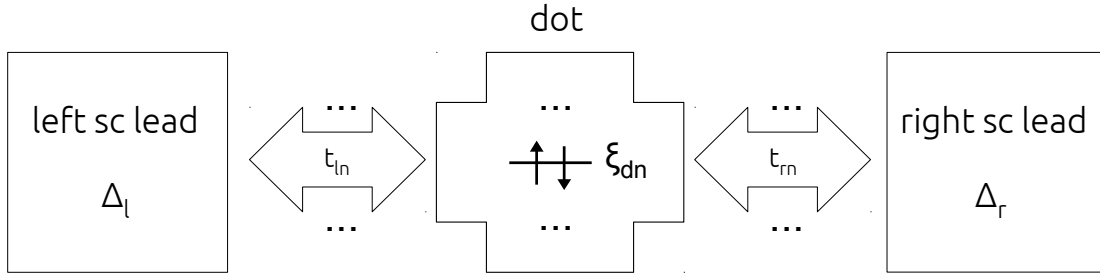


**Figure 5:** The superconductor/quantum-dot/superconductor system. The dot consists of  $N$  levels with energies  $\xi_{dn\sigma}$ . For non-interacting electrons those level energies are spin-independent. A gate voltage can shift the dot levels. The left and right lead are coupled with the dot via the terms  $t_{\alpha n}$ , where each level is coupled individually. The superconducting leads are determined by their gap energies  $\Delta_\alpha$ . There is a phase difference between the leads, which causes the supercurrent.

## 4 Transport in superconductor —quantum-dot junctions

We study the quantum transport of a system of a quantum dot confined between two superconducting leads, as illustrated in Fig. 5.

The superconductors are described by the BCS mean-field theory as it was introduced in Section 2. They are determined by their gap parameters. Furthermore, there is a phase difference between the superconducting leads, that causes a supercurrent.

The quantum dot is a confined region between the superconductors and couples to each of them on both sides. The dot has a total of  $N$  energy levels, which we will specify later. Due to the Pauli principle there can be a total of 2 electrons with opposite spin on each level. Even though interactions play an important role for the transport through nanostructures (especially Coulomb interactions), the electrons in the dot of our model are assumed to be noninteracting. The dot levels can be shifted by applying a gate voltage.

We aim to find the spectral function for the dot to find the Andreev bound states and to see how they depend on other parameters. Furthermore, we are going to calculate the supercurrent that runs through the system. Therefore, we will have to calculate the system's Green functions first.

### 4.1 Model Hamiltonian

The Hamiltonian for our system is given by

$$H = H_d + H_{\text{BCS}}^{\text{MF}} + H_{\text{hyb}}. \quad (4.1)$$

The Hamiltonian of the dot is

$$H_d = \sum_{n\sigma} \xi_{dn\sigma} d_{n\sigma}^\dagger d_{n\sigma}, \quad (4.2)$$

where the summation runs over all dot levels, which are of the energy  $\xi_{dn\sigma}$ . The level energies are labeled with the electron spin  $\sigma = \uparrow, \downarrow$ . For non-interacting electrons, the levels are independent of spin, but we will keep the label for a later discussion. Here, we also introduced the operators for the dot,  $d_{n\sigma}^\dagger$  and  $d_{n\sigma}$ , which create or annihilate an electron with spin  $\sigma$  on the  $n$ -th dot level.

The Hamiltonian for the superconducting leads is given by the mean-field BCS Hamiltonian, which was introduced in Eq. (2.7),

$$H_{\text{BCS}}^{\text{MF}} = \sum_{\mathbf{k}\alpha\sigma} \xi_{\mathbf{k}\alpha} c_{\mathbf{k}\alpha\sigma}^\dagger c_{\mathbf{k}\alpha\sigma} - \sum_{\mathbf{k}\alpha} \Delta_\alpha c_{\mathbf{k}\alpha\uparrow}^\dagger c_{-\mathbf{k}\alpha\downarrow}^\dagger - \sum_{\mathbf{k}\alpha} \Delta_\alpha^* c_{-\mathbf{k}\alpha\downarrow} c_{\mathbf{k}\alpha\uparrow}, \quad (4.3)$$

Recall, how the gap energy was defined in Eq. (2.8) with the constant coupling strength, Eq. (2.2). Therefore, the gap energy  $\Delta_\alpha$  is  $\mathbf{k}$  independent and only carries the lead index here, where  $\alpha$  denotes the left ( $l$ ) or right ( $r$ ) lead. Note that we could easily add more leads to the system just by extending the sum. For a normal lead the gap energy would then be zero.

The third part of the Hamiltonian for our system is the hybridization term,

$$\begin{aligned} H_{\text{hyb}} &= \sum_{\mathbf{k}\alpha n\sigma} \left( t_{\alpha n} c_{\mathbf{k}\alpha\sigma}^\dagger d_{n\sigma} + t_{\alpha n}^* d_{n\sigma}^\dagger c_{\mathbf{k}\alpha\sigma} \right) \\ &= \sum_{\mathbf{k}\alpha n\sigma} t_{\alpha n} c_{\mathbf{k}\alpha\sigma}^\dagger d_{n\sigma} + \text{h.c.}, \end{aligned} \quad (4.4)$$

The terms  $t_{\alpha n}$  describe the mixing of the dot and lead particles. Each dot level is coupled individually with the superconducting leads. The first term of the Hamiltonian gives the transfer of a dot electron to one of the leads. The hermitian conjugate describes the opposite direction.

#### 4.1.1 Nambu representation

We would like to rewrite the Hamiltonian by working in Nambu space. Therefore, we introduce the so-called Nambu spinors for the lead and dot particles,

$$\alpha_{\mathbf{k}\alpha} := \begin{pmatrix} c_{\mathbf{k}\alpha\uparrow} \\ c_{-\mathbf{k}\alpha\downarrow}^\dagger \end{pmatrix}, \quad \alpha_{dn} := \begin{pmatrix} d_{n\uparrow} \\ d_{n\downarrow}^\dagger \end{pmatrix}. \quad (4.5)$$

We can rewrite the Hamiltonian with the help of these spinors. We thus include particle-hole symmetry in our Hamiltonian. Rewriting then gives a matrix structure for  $H$ , where the three parts look as follows,

$$H_d = \sum_n \begin{pmatrix} d_{n\uparrow}^\dagger & d_{n\downarrow} \end{pmatrix} \begin{pmatrix} \xi_{dn\uparrow} & 0 \\ 0 & -\xi_{dn\downarrow} \end{pmatrix} \begin{pmatrix} d_{n\uparrow} \\ d_{n\downarrow}^\dagger \end{pmatrix} + \text{const.}, \quad (4.6)$$

$$H_{\text{BCS}}^{\text{MF}} = \sum_{\mathbf{k}\alpha} \begin{pmatrix} c_{\mathbf{k}\alpha\uparrow}^\dagger & c_{-\mathbf{k}\alpha\downarrow} \end{pmatrix} \begin{pmatrix} \xi_{\mathbf{k}\alpha} & -\Delta_\alpha \\ -\Delta_\alpha^* & -\xi_{\mathbf{k}\alpha} \end{pmatrix} \begin{pmatrix} c_{\mathbf{k}\alpha\uparrow} \\ c_{-\mathbf{k}\alpha\downarrow}^\dagger \end{pmatrix} + \text{const.}, \quad (4.7)$$

$$H_{\text{hyb}} = \sum_{\mathbf{k}\alpha n} \begin{pmatrix} c_{\mathbf{k}\alpha\uparrow}^\dagger & c_{-\mathbf{k}\alpha\downarrow} \end{pmatrix} \begin{pmatrix} t_{\alpha n} & 0 \\ 0 & -t_{\alpha n}^* \end{pmatrix} \begin{pmatrix} d_{n\uparrow} \\ d_{n\downarrow}^\dagger \end{pmatrix} + \text{h.c.} \quad (4.8)$$

The constant terms can be neglected as they do not give any contribution to the spectrum. The matrices in the Hamiltonians for the dot, the superconducting leads and the hybridization region are renamed as follows,

$$M_d^{(n)} = \begin{pmatrix} \xi_{dn\uparrow} & 0 \\ 0 & -\xi_{dn\downarrow} \end{pmatrix}, \quad (4.9)$$

$$M_{\text{sc}}^{(\mathbf{k}\alpha)} = \begin{pmatrix} \xi_{\mathbf{k}\alpha} & -\Delta_\alpha \\ -\Delta_\alpha^* & -\xi_{\mathbf{k}\alpha} \end{pmatrix} = \xi_{\mathbf{k}\alpha} m^3 - \Delta'_\alpha m^1 + \Delta''_\alpha m^2, \quad (4.10)$$

$$M_{\text{hyb}}^{(\alpha n)} = \begin{pmatrix} t_{\alpha n} & 0 \\ 0 & -t_{\alpha n}^* \end{pmatrix} = t'_{\alpha n} m^3 + it''_{\alpha n} m^0. \quad (4.11)$$

The matrices have been further expressed in terms of the identity matrix  $m^0 = \begin{pmatrix} 1 & 0 \\ 0 & 1 \end{pmatrix}$  as well as the Pauli matrices,

$$m^1 = \begin{pmatrix} 0 & 1 \\ 1 & 0 \end{pmatrix}, \quad m^2 = \begin{pmatrix} 0 & -i \\ i & 0 \end{pmatrix}, \quad m^3 = \begin{pmatrix} 1 & 0 \\ 0 & -1 \end{pmatrix}. \quad (4.12)$$

The gap energy is written with its real and imaginary part,  $\Delta_\alpha = \Delta'_\alpha + i\Delta''_\alpha$ , where  $\Delta'_\alpha$  is the real part and  $\Delta''_\alpha$  is the imaginary part of  $\Delta_\alpha$ . The same we do for the coupling term  $t_{\alpha n} = t'_{\alpha n} + it''_{\alpha n}$ . Thus, we can write our Hamiltonian in terms of the Nambu spinors and the newly introduced  $(2 \times 2)$ -matrices, which gives a more compact form,

$$H = \sum_n \alpha_{dn}^\dagger M_d^{(n)} \alpha_{dn} + \sum_{\mathbf{k}\alpha} \alpha_{\mathbf{k}\alpha}^\dagger M_{sc}^{(\mathbf{k}\alpha)} \alpha_{\mathbf{k}\alpha} + \sum_{\mathbf{k}\alpha n} \left( \alpha_{\mathbf{k}\alpha}^\dagger M_{hyb}^{(\alpha n)} \alpha_{dn} + \text{h.c.} \right). \quad (4.13)$$

The Hamiltonian in terms of the matrix components looks as follows,

$$\begin{aligned} H = & \sum_{\eta\eta'} \sum_n \alpha_{dn,\eta}^\dagger M_{d,\eta\eta'}^{(n)} \alpha_{dn,\eta'} + \sum_{\eta\eta'} \sum_{\mathbf{k}\alpha} \alpha_{\mathbf{k}\alpha,\eta}^\dagger M_{sc,\eta\eta'}^{(\mathbf{k}\alpha)} \alpha_{\mathbf{k}\alpha,\eta'} \\ & + \sum_{\eta\eta'} \sum_{\mathbf{k}\alpha n} \left( \alpha_{\mathbf{k}\alpha,\eta}^\dagger M_{hyb,\eta\eta'}^{(\alpha n)} \alpha_{dn,\eta'} + \alpha_{dn,\eta}^\dagger M_{hyb,\eta'\eta}^{(\alpha n)*} \alpha_{\mathbf{k}\alpha,\eta'} \right), \end{aligned} \quad (4.14)$$

with the Nambu indices  $\eta, \eta' = 1, 2$ .

## 4.2 The system's Green functions

We want to derive the single-particle Green functions for our system, which we introduced in Section 3.1. We first calculate the Matsubara Green functions with the help of the equation of motion technique. We can define Green functions for the three different parts of our system, i.e., the dot, the leads and the coupling region. The Green functions will be defined in terms of the Nambu spinors, which gives  $(2 \times 2)$ -matrix Green functions. Therefore, the Green functions will reveal particle-hole symmetry for our system.

Let us first write down the time derivatives for the Nambu spinors in the imaginary time formalism. Remember how the time derivative of operators in the Heisenberg picture for imaginary times looks like, Eq. (3.95). So we have to build the commutators with the Hamiltonian and find the derivative of the Nambu spinors for lead and dot particles is as follows,

$$\partial_\tau \alpha_{\mathbf{k}\alpha,\eta}(\tau) = - \sum_{\eta''} M_{sc,\eta\eta''}^{(\mathbf{k}\alpha)} \alpha_{\mathbf{k}\alpha,\eta''}(\tau) - \sum_{m\eta''} M_{hyb,\eta\eta''}^{(\alpha m)} \alpha_{dm,\eta''}(\tau), \quad (4.15)$$

$$\partial_\tau \alpha_{\mathbf{k}\alpha,\eta}^\dagger(\tau) = \sum_{\eta''} M_{sc,\eta''\eta}^{(\mathbf{k}\alpha)} \alpha_{\mathbf{k}\alpha,\eta''}^\dagger(\tau) + \sum_{m\eta''} M_{hyb,\eta\eta''}^{(\alpha m)*} \alpha_{dm,\eta''}^\dagger(\tau), \quad (4.16)$$

$$\partial_\tau \alpha_{dm,\eta}(\tau) = - \sum_{\eta''} M_{d,\eta\eta''}^{(m)} \alpha_{dm,\eta''}(\tau) - \sum_{\mathbf{k}\alpha} \sum_{\eta''} M_{hyb,\eta''\eta}^{(\alpha m)*} \alpha_{\mathbf{k}\alpha,\eta''}(\tau), \quad (4.17)$$

$$\partial_\tau \alpha_{dm,\eta}^\dagger(\tau) = \sum_{\eta''} M_{d,\eta''\eta}^{(m)} \alpha_{dm,\eta''}^\dagger(\tau) + \sum_{\mathbf{k}\alpha} \sum_{\eta''} M_{hyb,\eta''\eta}^{(\alpha m)} \alpha_{\mathbf{k}\alpha,\eta''}^\dagger(\tau). \quad (4.18)$$

The notation is here chosen componentwise in terms of the Nambu indices. For the commutators with the Hamiltonian, we used the anti-commutation relations for the Nambu spinors,

$$\begin{aligned} \{\alpha_{\mathbf{k}\alpha,\eta}(\tau), \alpha_{\mathbf{k}'\alpha',\eta'}(\tau')\} &= 0, \quad \{\alpha_{\mathbf{k}\alpha,\eta}^\dagger(\tau), \alpha_{\mathbf{k}'\alpha',\eta'}^\dagger(\tau')\} = 0, \\ \{\alpha_{\mathbf{k}\alpha,\eta}(\tau), \alpha_{\mathbf{k}'\alpha',\eta'}^\dagger(\tau')\} &= \delta(\tau - \tau') \delta_{\mathbf{k}\mathbf{k}'} \delta_{\alpha\alpha'} \delta_{\eta\eta'}, \end{aligned} \quad (4.19)$$

$$\begin{aligned} \{\alpha_{dm,\eta}(\tau), \alpha_{dn,\eta'}(\tau')\} &= 0, \quad \{\alpha_{dm,\eta}^\dagger(\tau), \alpha_{dn,\eta'}^\dagger(\tau')\} = 0, \\ \{\alpha_{dm,\eta}(\tau), \alpha_{dn,\eta'}^\dagger(\tau')\} &= \delta(\tau - \tau') \delta_{mn} \delta_{\eta\eta'}. \end{aligned} \quad (4.20)$$

Furthermore, operators for lead and dot particles always anti-commute with each other.

### 4.2.1 Matsubara Green function for the leads

The Matsubara Green function for the superconducting leads is defined according Eq. (3.85),

$$\mathcal{G}_{\mathbf{k}\alpha,\mathbf{k}'\alpha';\eta\eta'}(\tau) = -\langle T_\tau \alpha_{\mathbf{k}\alpha,\eta}(\tau) \alpha_{\mathbf{k}'\alpha',\eta'}^\dagger(0) \rangle. \quad (4.21)$$

Its derivative with respect to  $\tau$  is as in Eq. (3.94),

$$\partial_\tau \mathcal{G}_{\mathbf{k}\alpha,\mathbf{k}'\alpha';\eta\eta'}(\tau) = -\delta(\tau) \langle \{\alpha_{\mathbf{k}\alpha,\eta}(\tau), \alpha_{\mathbf{k}'\alpha',\eta'}^\dagger(0)\} \rangle - \langle T_\tau \partial_\tau \alpha_{\mathbf{k}\alpha,\eta}(\tau) \alpha_{\mathbf{k}'\alpha',\eta'}^\dagger(0) \rangle. \quad (4.22)$$

Using the anti-commutation relations as well as the time derivative of the lead particle Nambu operator from Eq. (4.15) gives,

$$\begin{aligned} \partial_\tau \mathcal{G}_{\mathbf{k}\alpha,\mathbf{k}'\alpha';\eta\eta'}(\tau) &= -\delta(\tau) \delta_{\mathbf{k}\mathbf{k}'} \delta_{\alpha\alpha'} \delta_{\eta\eta'} + \sum_{\eta''} M_{sc,\eta\eta''}^{(\mathbf{k}\alpha)} \langle T_\tau \alpha_{\mathbf{k}\alpha,\eta''}(\tau) \alpha_{\mathbf{k}'\alpha',\eta'}^\dagger(0) \rangle \\ &+ \sum_{m\eta''} M_{hyb,\eta\eta''}^{(\alpha m)} \langle T_\tau \alpha_{dm,\eta''}(\tau) \alpha_{\mathbf{k}'\alpha',\eta'}^\dagger(0) \rangle. \end{aligned} \quad (4.23)$$

We can identify one term from this expression as the leads Green function. Another term represents the Matsubara Green function for the hybridization of lead and dot. For the coupling of lead  $\alpha$  with the  $m$ -th dot level, it is defined as follows,

$$\mathcal{G}_{dm,\mathbf{k}'\alpha';\eta\eta'}(\tau) = -\langle T_\tau \alpha_{dm,\eta}(\tau) \alpha_{\mathbf{k}'\alpha',\eta'}^\dagger(0) \rangle. \quad (4.24)$$

Consequently, we can write Eq. (4.23) in terms of the Green functions,

$$\begin{aligned} \partial_\tau \mathcal{G}_{\mathbf{k}\alpha,\mathbf{k}'\alpha';\eta\eta'}(\tau) &= -\delta(\tau) \delta_{\mathbf{k}\mathbf{k}'} \delta_{\alpha\alpha'} \delta_{\eta\eta'} + \sum_{\eta''} M_{sc,\eta\eta''}^{(\mathbf{k}\alpha)} \mathcal{G}_{\mathbf{k}\alpha,\mathbf{k}'\alpha';\eta''\eta'}(\tau) \\ &+ \sum_{m\eta''} M_{hyb,\eta\eta''}^{(\alpha m)} \mathcal{G}_{dm,\mathbf{k}'\alpha';\eta''\eta'}(\tau). \end{aligned} \quad (4.25)$$

It is now nice to write this equation in matrix form in Nambu space,

$$\partial_\tau \mathcal{G}_{\mathbf{k}\alpha,\mathbf{k}'\alpha'}(\tau) = -\delta(\tau) \delta_{\mathbf{k}\mathbf{k}'} \delta_{\alpha\alpha'} m^0 - M_{sc}^{(\mathbf{k}\alpha)} \mathcal{G}_{\mathbf{k}\alpha,\mathbf{k}'\alpha'}(\tau) - \sum_m M_{hyb}^{(\alpha m)} \mathcal{G}_{dm,\mathbf{k}'\alpha'}(\tau). \quad (4.26)$$

Fourier transformation yields,

$$-i\omega_l \mathcal{G}_{\mathbf{k}\alpha,\mathbf{k}'\alpha'}(i\omega_l) = -\delta_{\mathbf{k}\mathbf{k}'} \delta_{\alpha\alpha'} m^0 - M_{sc}^{(\mathbf{k}\alpha)} \mathcal{G}_{\mathbf{k}\alpha,\mathbf{k}'\alpha'}(i\omega_l) - \sum_m M_{hyb}^{(\alpha m)} \mathcal{G}_{dm,\mathbf{k}'\alpha'}(i\omega_l), \quad (4.27)$$

where we denoted the index of the Matsubara frequencies with an  $l$  to not to get confused with the dot level numbers. Reordering gives

$$\delta_{\mathbf{k}\mathbf{k}'} \delta_{\alpha\alpha'} m^0 = \left( i\omega_l m^0 - M_{sc}^{(\mathbf{k}\alpha)} \right) \mathcal{G}_{\mathbf{k}\alpha,\mathbf{k}'\alpha'}(i\omega_l) - \sum_m M_{hyb}^{(\alpha m)} \mathcal{G}_{dm,\mathbf{k}'\alpha'}(i\omega_l). \quad (4.28)$$

We can identify the Matsubara lead Green function for the unperturbed system as

$$\begin{aligned} \mathbf{g}_{\mathbf{k}\alpha}(i\omega_l) &= \left( i\omega_l m^0 - M_{sc}^{(\mathbf{k}\alpha)} \right)^{-1} \\ &= \frac{i\omega_l m^0 + \xi_{\mathbf{k}\alpha} m^3 - \Delta'_\alpha m^1 + \Delta''_\alpha m^2}{(i\omega_l)^2 - (\xi_{\mathbf{k}\alpha}^2 + |\Delta_\alpha|^2)}, \end{aligned} \quad (4.29)$$

which is exactly the case when the leads are not coupled to the dot, i.e., if for all  $m$  it is  $M_{hyb}^{(\alpha m)} = 0$ . Thus, we obtain the Matsubara Green function for the leads of our system,

$$\mathcal{G}_{\mathbf{k}\alpha,\mathbf{k}'\alpha'}(i\omega_l) = \delta_{\mathbf{k}\mathbf{k}'} \delta_{\alpha\alpha'} \mathbf{g}_{\mathbf{k}\alpha}(i\omega_l) + \mathbf{g}_{\mathbf{k}\alpha}(i\omega_l) \sum_m M_{hyb}^{(\alpha m)} \mathcal{G}_{dm,\mathbf{k}'\alpha'}(i\omega_l). \quad (4.30)$$

#### 4.2.2 Hybridization Matsubara Green function

We would like to determine the Green function for the coupling region of our system now. There are two Green functions of that kind. The first one has been defined in Eq. (4.24). We would like to do a small adjustment here, from which we will benefit in a later consideration. In Eq. (3.84) we showed that the Green functions only depend on the time difference. Thus we can shift the times, such that we can write Eq. (4.24) as

$$\mathcal{G}_{dm,\mathbf{k}\alpha;\eta\eta'}(\tau) = -\langle T_\tau \alpha_{dm,\eta}(0) \alpha_{\mathbf{k}\alpha,\eta'}^\dagger(-\tau) \rangle. \quad (4.31)$$

Differentiation with respect to  $\tau$  gives

$$\partial_\tau \mathcal{G}_{dm, \mathbf{k}\alpha; \eta\eta'}(\tau) = -\langle T_\tau \alpha_{dm, \eta}(0) \partial_\tau \alpha_{\mathbf{k}\alpha, \eta'}^\dagger(-\tau) \rangle \quad (4.32)$$

$$\begin{aligned} &= \sum_{\eta''} M_{sc, \eta''\eta'}^{(\mathbf{k}\alpha)} \langle T_\tau \alpha_{dm, \eta}(0) \alpha_{\mathbf{k}\alpha, \eta''}^\dagger(-\tau) \rangle \\ &\quad + \sum_{n\eta''} M_{hyb, \eta''\eta'}^{(\alpha n)*} \langle T_\tau \alpha_{dm, \eta}(0) \alpha_{dn, \eta''}^\dagger(-\tau) \rangle \end{aligned} \quad (4.33)$$

$$= -\sum_{\eta''} \mathcal{G}_{dm, \mathbf{k}\alpha; \eta\eta''}(\tau) M_{sc, \eta''\eta'}^{(\mathbf{k}\alpha)} - \sum_{n\eta''} \mathcal{G}_{d, mn; \eta\eta''}(\tau) M_{hyb, \eta''\eta'}^{(\alpha n)*}. \quad (4.34)$$

Here, we shifted back the times, then we identified again the hybridization Green function as well as the Green function for the dot,  $\mathcal{G}_{d, mn}(\tau)$ , which will be defined in the next section. The matrix form of Eq. (4.34) looks as follows,

$$\partial_\tau \mathcal{G}_{dm, \mathbf{k}\alpha}(\tau) = -\mathcal{G}_{dm, \mathbf{k}\alpha}(\tau) M_{sc}^{(\mathbf{k}\alpha)} - \sum_n \mathcal{G}_{d, mn}(\tau) M_{hyb}^{(\alpha n)\dagger}. \quad (4.35)$$

After Fourier transformation we find the hybridization Green function,

$$\mathcal{G}_{dm, \mathbf{k}\alpha}(i\omega_l) = \sum_n \mathcal{G}_{d, mn}(i\omega_l) M_{hyb}^{(\alpha n)\dagger} \mathbf{g}_{\mathbf{k}\alpha}(i\omega_l). \quad (4.36)$$

The second Matsubara Green function we can define for the coupled region is

$$\mathcal{G}_{\mathbf{k}\alpha, dm; \eta\eta'}(\tau) = -\langle T_\tau \alpha_{\mathbf{k}\alpha, \eta}(\tau) \alpha_{dm, \eta'}^\dagger(0) \rangle. \quad (4.37)$$

In principle, it describes the transport from lead  $\alpha$  to the dot level  $m$ , thus the opposite direction of  $\mathcal{G}_{dm, \mathbf{k}\alpha}$ . The equation of motion technique and Fourier transformation yields in matrix structure,

$$\mathcal{G}_{\mathbf{k}\alpha, dm}(i\omega_l) = \sum_n \mathbf{g}_{\mathbf{k}\alpha}(i\omega_l) M_{hyb}^{(\alpha n)} \mathcal{G}_{d, nm}(i\omega_l). \quad (4.38)$$

### 4.2.3 Matsubara Green function for the dot

The Matsubara Green function for the dot is defined as follows,

$$\mathcal{G}_{d, mn; \eta\eta'}(\tau) = -\langle T_\tau \alpha_{dm, \eta}(\tau) \alpha_{dn, \eta'}^\dagger(0) \rangle. \quad (4.39)$$

The derivative with respect to  $\tau$  gives

$$\partial_\tau \mathcal{G}_{d, mn; \eta\eta'}(\tau) = -\delta(\tau) \langle \{ \alpha_{dm, \eta}(\tau), \alpha_{dn, \eta'}^\dagger(0) \} \rangle - \langle T_\tau \partial_\tau \alpha_{dm, \eta}(\tau) \alpha_{dn, \eta'}^\dagger(0) \rangle. \quad (4.40)$$

Next we insert the time derivative for the Nambu operator of the dot electrons, Eq. (4.17), thus

$$\begin{aligned} \partial_\tau \mathcal{G}_{d, mn; \eta\eta'}(\tau) &= -\delta(\tau) \delta_{mn} \delta_{\eta\eta'} + \sum_{\eta''} M_{d, \eta\eta''}^{(m)} \langle T_\tau \alpha_{dm, \eta''}(\tau) \alpha_{dn, \eta'}^\dagger(0) \rangle \\ &\quad + \sum_{\mathbf{k}\alpha} \sum_{\eta''} M_{hyb, \eta''\eta}^{(\alpha m)*} \langle T_\tau \alpha_{\mathbf{k}\alpha, \eta''}(\tau) \alpha_{dn, \eta'}^\dagger(0) \rangle. \end{aligned} \quad (4.41)$$

We find again the dot Green function and the hybridization Green function in this equation. In matrix form we obtain

$$\partial_\tau \mathcal{G}_{d, mn}(\tau) = -\delta(\tau) \delta_{mn} m^0 - M_d^{(m)} \mathcal{G}_{d, mn}(\tau) - \sum_{\mathbf{k}\alpha} M_{hyb}^{(\alpha m)\dagger} \mathcal{G}_{\mathbf{k}\alpha, dn}(\tau). \quad (4.42)$$

The Fourier transformation of this is

$$-i\omega_l \mathcal{G}_{d,mn}(i\omega_l) = -\delta_{mn} m^0 - M_d^{(m)} \mathcal{G}_{d,mn}(i\omega_l) - \sum_{\mathbf{k}\alpha} M_{\text{hyb}}^{(\alpha m)\dagger} \mathcal{G}_{\mathbf{k}\alpha,dn}(i\omega_l). \quad (4.43)$$

A little rearrangement gives

$$\delta_{mn} m^0 = (i\omega_l m^0 - M_d^{(m)}) \mathcal{G}_{d,mn}(i\omega_l) - \sum_{\mathbf{k}\alpha} M_{\text{hyb}}^{(\alpha m)\dagger} \mathcal{G}_{\mathbf{k}\alpha,dn}(i\omega_l). \quad (4.44)$$

For the case that  $M_{\text{hyb}}^{(\alpha m)\dagger} = 0$  for all  $m$ , we get the Matsubara dot Green function for the unperturbed system,

$$\begin{aligned} \mathbf{g}_{d,mm}(i\omega_l) &= \left( i\omega_l m^0 - M_d^{(m)} \right)^{-1} \\ &= \begin{pmatrix} \frac{1}{i\omega_l - \xi_{dm\uparrow}} & 0 \\ 0 & \frac{1}{i\omega_l + \xi_{dm\downarrow}} \end{pmatrix}. \end{aligned} \quad (4.45)$$

This can be used together with the hybridization Green function we found in Eq. (4.38), then Eq. (4.44) yields

$$\delta_{mn} m^0 = \mathbf{g}_{d,mm}^{-1}(i\omega_l) \mathcal{G}_{d,mn}(i\omega_l) - \sum_{\mathbf{k}\alpha p} M_{\text{hyb}}^{(\alpha m)\dagger} \mathbf{g}_{\mathbf{k}\alpha}(i\omega_l) M_{\text{hyb}}^{(\alpha p)} \mathcal{G}_{d,pn}(i\omega_l), \quad (4.46)$$

where  $p$  is just another dot level index. Let us do one further identification. In Eq. (4.46) we find the so-called *self-energy* in the imaginary time formalism as

$$\begin{aligned} \tilde{\Sigma}_{d,mp}(i\omega_l) &= \sum_{\alpha} \tilde{\Sigma}_{d,mp}^{(\alpha)}(i\omega_l) \\ &= \sum_{\mathbf{k}\alpha} M_{\text{hyb}}^{(\alpha m)\dagger} \mathbf{g}_{\mathbf{k}\alpha}(i\omega_l) M_{\text{hyb}}^{(\alpha p)}. \end{aligned} \quad (4.47)$$

We then rewrite Eq. (4.46) in terms of the self-energy,

$$\delta_{mn} m^0 = \mathbf{g}_{d,mm}^{-1}(i\omega_l) \mathcal{G}_{d,mn}(i\omega_l) - \sum_p \tilde{\Sigma}_{d,mp}(i\omega_l) \mathcal{G}_{d,pn}(i\omega_l). \quad (4.48)$$

Since  $\mathbf{g}_{d,mm}^{-1}(i\omega_l)$  is diagonal, this gives another matrix equation in the basis of the dot levels. This means, if we have an  $N$ -level dot, the dot Green functions and the self energy for the dot are in fact  $(2N \times 2N)$ -matrices, or  $(N \times N)$ -matrices where each entry is a  $(2 \times 2)$ -matrix in Nambu space. Thus, the Green functions in the space of the dot levels look as follows for an  $N$ -level dot,

$$\mathcal{G}_d = \begin{pmatrix} \mathcal{G}_{d,11} & \mathcal{G}_{d,12} & \cdots & \mathcal{G}_{d,1N} \\ \mathcal{G}_{d,21} & \mathcal{G}_{d,22} & & \vdots \\ \vdots & & \ddots & \\ \mathcal{G}_{d,N1} & \cdots & & \mathcal{G}_{d,NN} \end{pmatrix}, \quad (4.49)$$

where each matrix element can be written as a  $(2 \times 2)$ -Nambu matrix,

$$\mathcal{G}_{d,mn} = \begin{pmatrix} \mathcal{G}_{d,mn;11} & \mathcal{G}_{d,mn;12} \\ \mathcal{G}_{d,mn;21} & \mathcal{G}_{d,mn;22} \end{pmatrix}. \quad (4.50)$$

To not to get confused with the indices, we will separate the dot level indices from the Nambu indices with a semicolon as shown here.

In this notation, Eq. (4.48) turns to

$$\mathbb{1} = \mathbf{g}_d^{-1}(i\omega_l)\mathcal{G}_d(i\omega_l) - \sum_p \tilde{\Sigma}_d(i\omega_l)\mathcal{G}_d(i\omega_l), \quad (4.51)$$

which we can solve for the Matsubara dot Green function,

$$\mathcal{G}_d^{-1}(i\omega_l) = \mathbf{g}_d^{-1}(i\omega_l) - \tilde{\Sigma}_d(i\omega_l). \quad (4.52)$$

With Eq. (4.52) we are now able to calculate the dot Green function for any number of levels. We just have to think of the unperturbed Green function as a diagonal matrix, for which every entry is defined as

$$\mathbf{g}_{d,mn}(i\omega_l) = \delta_{mn} \begin{pmatrix} \frac{1}{i\omega_l - \xi_{dm\uparrow}} & 0 \\ 0 & \frac{1}{i\omega_l + \xi_{dm\downarrow}} \end{pmatrix}. \quad (4.53)$$

The entries of the self-energy were defined in Eq. (4.47). We can perform the sum over the unperturbed Green function for lead  $\alpha$ , Eq. (4.29), by changing momentum summation to energy integration,  $\sum_{\mathbf{k}} \Rightarrow \int d\xi_{\mathbf{k}\alpha} \nu_F^\alpha$ , with the constant density of states  $\nu_F^\alpha$ ,

$$\begin{aligned} \sum_{\mathbf{k}} \mathbf{g}_{\mathbf{k}\alpha}(i\omega_l) &= \nu_F^\alpha \int d\xi_{\mathbf{k}\alpha} \mathbf{g}_{\mathbf{k}\alpha}(i\omega_l) \\ &= \nu_F^\alpha \int d\xi_{\mathbf{k}\alpha} \frac{-i\omega_l m^0 - \xi_{\mathbf{k}\alpha} m^3 + \Delta'_\alpha m^1 - \Delta''_\alpha m^2}{-(i\omega_l)^2 + \xi_{\mathbf{k}\alpha}^2 + |\Delta_\alpha|^2} \\ &= -\frac{\pi \nu_F^\alpha}{E_\alpha(i\omega_l)} (i\omega_l m^0 - \Delta'_\alpha m^1 + \Delta''_\alpha m^2), \end{aligned} \quad (4.54)$$

where we defined  $E_\alpha(i\omega_l) = \sqrt{|\Delta_\alpha|^2 - (i\omega_l)^2}$ . To perform the integral we used the following relations,

$$\int_{-b}^b \frac{dx}{a^2 + x^2} = \frac{2}{a} \arctan\left(\frac{b}{a}\right) = \frac{\pi}{a}, \quad \text{for } b \rightarrow \infty, \quad (4.55)$$

$$\int_{-b}^b \frac{xdx}{a^2 + x^2} = 0. \quad (4.56)$$

This gives the following expression for the self-energy,

$$\begin{aligned} \tilde{\Sigma}_{d,mn}(i\omega_l) &= \sum_{\alpha} \tilde{\Sigma}_{d,mn}^{(\alpha)}(i\omega_l) = \sum_{\mathbf{k}\alpha} M_{\text{hyb}}^{(\alpha m)\dagger} \mathbf{g}_{\mathbf{k}\alpha}(i\omega_l) M_{\text{hyb}}^{(\alpha n)} \\ &= -\sum_{\alpha} \frac{\pi \nu_F^\alpha}{E_\alpha(i\omega_l)} \begin{pmatrix} t_{\alpha m}^* t_{\alpha n} i\omega_l & t_{\alpha m}^* t_{\alpha n}^* \Delta_\alpha \\ t_{\alpha m} t_{\alpha n} \Delta_\alpha^* & t_{\alpha m} t_{\alpha n}^* i\omega_l \end{pmatrix}. \end{aligned} \quad (4.57)$$

Recall, how the  $M_{\text{hyb}}^{(\alpha n)}$ -matrices were defined for the Hamiltonian, Eq. (4.11).

#### 4.2.4 Retarded and advanced Green functions

Having found the Matsubara Green functions, we are now able to determine the retarded and advanced Green functions via analytic continuation, according to Eqs. (3.100) and (3.101). Thereby, the self-energy we found for the dot must be analytic continued likewise. The retarded and advanced functions

are denoted for the dot as follows,

$$G_{d,mn}^{R/A}(\omega) = \mathcal{G}_{d,mn}(i\omega_l \rightarrow \omega \pm i\eta), \quad (4.58)$$

$$g_{d,mn}^{R/A}(\omega) = \delta_{mn} \mathbf{g}_{d,mm}(i\omega_l \rightarrow \omega \pm i\eta), \quad (4.59)$$

$$\Sigma_{d,mn}^{R/A}(\omega) = \tilde{\Sigma}_{d,mn}(i\omega_l \rightarrow \omega \pm i\eta). \quad (4.60)$$

For the leads they are

$$g_{\mathbf{k}\alpha}^{R/A}(\omega) = \mathbf{g}_{\mathbf{k}\alpha}(i\omega_l \rightarrow \omega \pm i\eta), \quad (4.61)$$

$$G_{\mathbf{k}\alpha, \mathbf{k}'\alpha'}^{R/A}(\omega) = \mathcal{G}_{\mathbf{k}\alpha, \mathbf{k}'\alpha'}(i\omega_l \rightarrow \omega \pm i\eta), \quad (4.62)$$

and the retarded and advanced hybridization Green functions are

$$G_{\mathbf{k}\alpha, dm}^{R/A}(\omega) = \mathcal{G}_{\mathbf{k}\alpha, dm}(i\omega_l \rightarrow \omega \pm i\eta), \quad (4.63)$$

$$G_{dm, \mathbf{k}\alpha}^{R/A}(\omega) = \mathcal{G}_{dm, \mathbf{k}\alpha}(i\omega_l \rightarrow \omega \pm i\eta). \quad (4.64)$$

### 4.3 Derivation of the current

We would like to calculate the current for our system now. The calculations are according to [10,11], where they calculate the current in a N-QD-N system by means of the nonequilibrium Green function technique. There, one encounters the contour-ordered Green functions, that have been introduced in Section 3.5.

The current in lead  $\alpha$  is given by the time evolution of the average occupation number operator for  $\alpha$ . The time evolution is then given by the time derivative for Heisenberg operators, i.e., by commutation with the Hamiltonian,

$$\begin{aligned} J_\alpha &= -e\langle \dot{N}_\alpha \rangle \\ &= -\frac{ie}{\hbar} \langle [H, N_\alpha] \rangle, \end{aligned} \quad (4.65)$$

The occupation number operator is given by

$$N_\alpha = \sum_{\mathbf{k}\sigma} c_{\mathbf{k}\alpha\sigma}^\dagger c_{\mathbf{k}\alpha\sigma}. \quad (4.66)$$

This can also be expressed in Nambu space,

$$N_\alpha = \sum_{\mathbf{k}} \alpha_{\mathbf{k}\alpha}^\dagger m^3 \alpha_{\mathbf{k}\alpha} \quad (4.67)$$

$$= \sum_{\mathbf{k}, \nu\nu'} \alpha_{\mathbf{k}\alpha, \nu}^\dagger m_{\nu\nu'}^3 \alpha_{\mathbf{k}\alpha, \nu'}, \quad (4.68)$$

where  $\nu, \nu'$  are Nambu indices and  $m^3$  is a Pauli matrix, Eq. (4.12). The commutator of  $N_\alpha$  and the Hamiltonian as it is given in Eq. (4.14), yields

$$\begin{aligned} J_\alpha &= -\frac{ie}{\hbar} \sum_{\mathbf{k}n} \sum_{\eta\eta'} m_{\eta\eta'}^3 2M_{\Delta, \eta'\eta}^{(\alpha)} \langle \alpha_{\mathbf{k}\alpha, \eta'}^\dagger \alpha_{\mathbf{k}\alpha, \eta} \rangle \\ &\quad + \frac{ie}{\hbar} \sum_{\mathbf{k}n} \sum_{\eta} m_{\eta\eta}^3 \left[ M_{\text{hyb}, \eta\eta}^{(\alpha n)} \langle \alpha_{\mathbf{k}\alpha, \eta}^\dagger \alpha_{dn, \eta} \rangle - M_{\text{hyb}, \eta\eta}^{(\alpha n)*} \langle \alpha_{dn, \eta}^\dagger \alpha_{\mathbf{k}\alpha, \eta} \rangle \right], \end{aligned} \quad (4.69)$$

where  $M_{\Delta}^{(\alpha)} = -\Delta'_\alpha m^1 + \Delta''_\alpha m^2$ . Here we used the fact that  $M_{\text{hyb}}^{(\alpha n)}$  and  $m^3$  are diagonal, as well as the anti-commutation relations, Eqs. (4.19) and (4.20).

We notice here, that the first term of the current in Eq. (4.69) is an artifact due to the BCS mean-field approximation. Because of particle conservation, the commutator with the original BCS Hamiltonian, Eq. (2.1), should give zero in fact, i.e.,  $[H_{\text{BCS}}, N_\alpha] = 0$ . Therefore, we will drop this term. The current thus is

$$\begin{aligned} J_\alpha &= \frac{e}{\hbar} \sum_{\mathbf{k}n} \sum_{\eta} m_{\eta\eta}^3 \left[ iM_{\text{hyb}, \eta\eta}^{(\alpha n)} \langle \alpha_{\mathbf{k}\alpha, \eta}^\dagger \alpha_{dn, \eta} \rangle - iM_{\text{hyb}, \eta\eta}^{(\alpha n)*} \langle \alpha_{dn, \eta}^\dagger \alpha_{\mathbf{k}\alpha, \eta} \rangle \right] \\ &= \frac{e}{\hbar} \sum_{\mathbf{k}n} \sum_{\eta} \left[ iM_{\text{hyb}, \eta\eta}^{(\alpha n)} m_{\eta\eta}^3 \langle \alpha_{\mathbf{k}\alpha, \eta}^\dagger(t) \alpha_{dn, \eta}(t) \rangle + \text{h.c.} \right]. \end{aligned} \quad (4.70)$$

We identify the following lesser hybridization Green function in our current formula,

$$G_{dn, \mathbf{k}\alpha; \eta\eta'}^<(t-t') = i \langle \alpha_{\mathbf{k}\alpha, \eta'}^\dagger(t') \alpha_{dn, \eta}(t) \rangle. \quad (4.71)$$

Therefore, it is

$$J_\alpha = \frac{e}{\hbar} \sum_{\mathbf{kn}} \sum_{\eta} \left[ M_{\text{hyb},\eta\eta}^{(\alpha n)} m_{\eta\eta}^3 G_{dn,\mathbf{k}\alpha;\eta\eta}^<(t,t) + \text{h.c.} \right] \quad (4.72)$$

$$= \frac{e}{\hbar} \sum_{\mathbf{kn}} \text{Tr} \left\{ M_{\text{hyb}}^{(\alpha n)} m^3 G_{dn,\mathbf{k}\alpha}^<(t,t) + \text{h.c.} \right\}, \quad (4.73)$$

$$= \frac{2e}{\hbar} \sum_{\mathbf{kn}} \text{Tr} \left\{ \text{Re} \left[ M_{\text{hyb}}^{(\alpha n)} m^3 G_{dn,\mathbf{k}\alpha}^<(t,t) \right] \right\}. \quad (4.74)$$

Here we used again that  $M_{\text{hyb}}^{(\alpha n)}$  and  $m^3$  are diagonal matrices. Thus, the summation over the Nambu indices gives the trace of the matrix product. We further used that  $\text{Tr}\{A + A^\dagger\} = 2\text{Tr}\{\text{Re}[A]\}$ .

Since the Green function does only depend on the time difference, Fourier transformation gives,

$$J_\alpha = \frac{2e}{\hbar} \int \frac{d\omega}{2\pi} \sum_{\mathbf{kn}} \text{Tr} \left\{ \text{Re} \left[ M_{\text{hyb}}^{(\alpha n)} m^3 G_{dn,\mathbf{k}\alpha}^<(\omega) \right] \right\}. \quad (4.75)$$

We now want to calculate the lesser Green function for the hybridization of dot and lead,  $G_{dn,\mathbf{k}\alpha}^<(\omega)$ . To obtain a more general relationship between the Green function we use nonequilibrium Green function techniques here.

According to Haug and Jauho, we start from the (real) time-ordered Green function in equilibrium,

$$G_{dn,\mathbf{k}\alpha;\eta\eta'}^t(t-t') = -i\langle T\alpha_{dn,\eta}(t)\alpha_{\mathbf{k}\alpha,\eta'}^\dagger(t') \rangle. \quad (4.76)$$

Now we use the equation of motion technique and differentiate with respect to  $t'$ ,

$$\partial_{t'} G_{dn,\mathbf{k}\alpha;\eta\eta'}^t(t-t') = -i\langle T\alpha_{dn,\eta}(t)\partial_{t'}\alpha_{\mathbf{k}\alpha,\eta'}^\dagger(t') \rangle. \quad (4.77)$$

The time derivative of the operator is given via the commutator with the Hamiltonian, Eq. (4.14),

$$\begin{aligned} \partial_{t'}\alpha_{\mathbf{k}\alpha,\eta'}^\dagger(t') &= i[H, \alpha_{\mathbf{k}\alpha,\eta'}^\dagger](t') \\ &= i \sum_{\eta''} M_{sc,\eta''\eta'}^{(\mathbf{k}\alpha)} \alpha_{\mathbf{k}\alpha,\eta''}^\dagger(t') + i \sum_{m\eta''} M_{\text{hyb},\eta'\eta''}^{(\alpha m)*} \alpha_{dm,\eta''}^\dagger(t'). \end{aligned} \quad (4.78)$$

This gives

$$\partial_{t'} G_{dn,\mathbf{k}\alpha;\eta\eta'}^t(t-t') = \sum_{\eta''} M_{sc,\eta''\eta'}^{(\mathbf{k}\alpha)} \langle T\alpha_{dn,\eta}(t)\alpha_{\mathbf{k}\alpha,\eta''}^\dagger(t') \rangle + \sum_{m\eta''} M_{\text{hyb},\eta'\eta''}^{(\alpha m)*} \langle T\alpha_{dn,\eta}(t)\alpha_{dm,\eta''}^\dagger(t') \rangle. \quad (4.79)$$

In this expression, we can identify the time ordered hybridization Green function as well as the time ordered dot Green function,

$$G_{d,nm;\eta\eta'}^t(t-t') = -i\langle T\alpha_{dn,\eta}(t)\alpha_{dm,\eta'}^\dagger(t') \rangle. \quad (4.80)$$

Therefore, we get

$$-i\partial_{t'} G_{dn,\mathbf{k}\alpha;\eta\eta'}^t(t-t') = \sum_{\eta''} G_{dn,\mathbf{k}\alpha;\eta\eta''}^t(t-t') M_{sc,\eta''\eta'}^{(\mathbf{k}\alpha)} + \sum_{m\eta''} G_{d,nm;\eta\eta''}^t(t-t') M_{\text{hyb},\eta'\eta''}^{(\alpha m)*}, \quad (4.81)$$

or in matrix notation in Nambu space,

$$-i\partial_{t'} G_{dn,\mathbf{k}\alpha}^t(t-t') = G_{dn,\mathbf{k}\alpha}^t(t-t') M_{sc}^{(\mathbf{k}\alpha)} + \sum_m G_{d,nm}^t(t-t') M_{\text{hyb}}^{(\alpha m)\dagger}. \quad (4.82)$$

Fourier transformation of this equation gives

$$\omega G_{dn,\mathbf{k}\alpha}^t(\omega) = G_{dn,\mathbf{k}\alpha}^t(\omega) M_{sc}^{(\mathbf{k}\alpha)} + \sum_m G_{d,nm}^t(\omega) M_{hyb}^{(\alpha m)\dagger}. \quad (4.83)$$

If we solve this for the hybridization Green function, we get

$$G_{dn,\mathbf{k}\alpha}^t(\omega) = \sum_m G_{d,nm}^t(\omega) M_{hyb}^{(\alpha m)\dagger} \left( \omega m^0 - M_{sc}^{(\mathbf{k}\alpha)} \right)^{-1} \quad (4.84)$$

$$= \sum_m G_{d,nm}^t(\omega) M_{hyb}^{(\alpha m)\dagger} g_{\mathbf{k}\alpha}^t(\omega). \quad (4.85)$$

Here, we could identify the time-ordered Green function for the uncoupled lead  $\alpha$ , which looks similar to the result we found for the Matsubara Green function in Eq. (4.29). We shortly want to show that this is true.

$$\begin{aligned}
g_{\mathbf{k}\alpha;\eta\eta'}^t(t-t') &= -i \langle T \alpha_{\mathbf{k}\alpha,\eta}(t) \alpha_{\mathbf{k}\alpha,\eta'}^\dagger(t') \rangle \\
\partial_t g_{\mathbf{k}\alpha;\eta\eta'}^t(t-t') &= -i \delta(t-t') \delta_{\eta\eta'} - i \langle T \partial_t \alpha_{\mathbf{k}\alpha,\eta}(t) \alpha_{\mathbf{k}\alpha,\eta'}^\dagger(t') \rangle \\
\partial_t \alpha_{\mathbf{k}\alpha,\eta}(t) &= i [H_{BCS}^{MF}, \alpha_{\mathbf{k}\alpha,\eta}](t) \\
&= -i \sum_{\eta''} M_{sc,\eta\eta''}^{(\mathbf{k}\alpha)} \alpha_{\mathbf{k}\alpha,\eta''}(t) \\
\Rightarrow i \partial_t g_{\mathbf{k}\alpha;\eta\eta'}^t(t-t') &= \delta(t-t') \delta_{\eta\eta'} - i \sum_{\eta''} M_{sc,\eta\eta''}^{(\mathbf{k}\alpha)} \langle T \alpha_{\mathbf{k}\alpha,\eta''}(t) \alpha_{\mathbf{k}\alpha,\eta'}^\dagger(t') \rangle \\
&= \delta(t-t') \delta_{\eta\eta'} + \sum_{\eta''} M_{sc,\eta\eta''}^{(\mathbf{k}\alpha)} g_{\mathbf{k}\alpha;\eta''\eta'}^t(t-t') \\
\Rightarrow \omega g_{\mathbf{k}\alpha}^t(\omega) &= m^0 + M_{sc}^{(\mathbf{k}\alpha)} g_{\mathbf{k}\alpha}^t(\omega) \\
\Rightarrow g_{\mathbf{k}\alpha}^t(\omega) &= \left( \omega m^0 - M_{sc}^{(\mathbf{k}\alpha)} \right)^{-1}
\end{aligned} \quad (4.86)$$

We Fourier transform once again Eq. (4.85), therefore we use the relation shown in Eq. (A.5), so we obtain

$$G_{dn,\mathbf{k}\alpha}^t(t-t') = \sum_m \int dt_1 G_{d,nm}^t(t-t_1) M_{hyb}^{(\alpha m)\dagger} g_{\mathbf{k}\alpha}^t(t_1-t'). \quad (4.87)$$

In the nonequilibrium case, this equation has the same form, except that the integration runs on the contour and the time ordered functions are now contour ordered Green functions,

$$G_{dn,\mathbf{k}\alpha}^C(\tau, \tau') = \sum_m \int_C d\tau_1 G_{d,nm}^C(\tau, \tau_1) M_{hyb}^{(\alpha m)\dagger} g_{\mathbf{k}\alpha}^C(\tau_1, \tau'), \quad (4.88)$$

where we denoted  $\tau$  as times on the contour. To obtain from this the lesser Green function, we can use the Langreth rules, see Eq. (3.108). Thus, we get

$$G_{dn,\mathbf{k}\alpha}^<(t-t') = \sum_m \int dt_1 \left[ G_{d,nm}^R(t-t_1) M_{hyb}^{(\alpha m)\dagger} g_{\mathbf{k}\alpha}^<(t_1-t') + G_{d,nm}^<(t-t_1) M_{hyb}^{(\alpha m)\dagger} g_{\mathbf{k}\alpha}^A(t_1-t') \right]. \quad (4.89)$$

We Fourier transform one more time using again relation (A.5), which gives

$$G_{dn,\mathbf{k}\alpha}^<(\omega) = \sum_m \left[ G_{d,nm}^R(\omega) M_{hyb}^{(\alpha m)\dagger} g_{\mathbf{k}\alpha}^<(\omega) + G_{d,nm}^<(\omega) M_{hyb}^{(\alpha m)\dagger} g_{\mathbf{k}\alpha}^A(\omega) \right]. \quad (4.90)$$

This result is still valid for general systems. We now specialize on equilibrium systems, i.e., we can use the fluctuation-dissipation theorem, Eq. (3.79), to determine the lesser Green functions,

$$\begin{aligned} g_{\mathbf{k}\alpha}^<(\omega) &= in_F(\omega)A_{\mathbf{k}\alpha}(\omega) \\ &= -n_F(\omega)[g_{\mathbf{k}\alpha}^R(\omega) - g_{\mathbf{k}\alpha}^A(\omega)], \end{aligned} \quad (4.91)$$

$$\begin{aligned} G_{d,nm}^<(\omega) &= in_F(\omega)A_{d,nm}(\omega) \\ &= -n_F(\omega)[G_{d,nm}^R(\omega) - G_{d,nm}^A(\omega)], \end{aligned} \quad (4.92)$$

where the spectral function has been defined in Eq. (3.72) as the difference of retarded and advanced Green function. If we plug this back into Eq. (4.90), we obtain

$$G_{dn,\mathbf{k}\alpha}^<(\omega) = -n_F(\omega) \sum_m \left[ G_{d,nm}^R(\omega) M_{\text{hyb}}^{(\alpha m)\dagger} g_{\mathbf{k}\alpha}^R(\omega) - G_{d,nm}^A(\omega) M_{\text{hyb}}^{(\alpha m)\dagger} g_{\mathbf{k}\alpha}^A(\omega) \right]. \quad (4.93)$$

Thus, we have found the lesser Green function for the hybridization region. We already determined the retarded and advanced Matsubara Green functions for dot and lead and the real time Green function can be obtained by analytic continuation, as we showed in Eqs. (4.58)-(4.64).

The lesser Green function we just found can now be plugged into the current expression we had in Eq. (4.75), so that we get

$$J_\alpha = -\frac{2e}{\hbar} \int \frac{d\omega}{2\pi} n_F(\omega) \sum_{\mathbf{k}nm} \text{Tr} \left\{ \text{Re} \left[ M_{\text{hyb}}^{(\alpha n)} m^3 G_{d,nm}^R(\omega) M_{\text{hyb}}^{(\alpha m)\dagger} g_{\mathbf{k}\alpha}^R(\omega) - M_{\text{hyb}}^{(\alpha n)} m^3 G_{d,nm}^A(\omega) M_{\text{hyb}}^{(\alpha m)\dagger} g_{\mathbf{k}\alpha}^A(\omega) \right] \right\} \quad (4.94)$$

$$= -\frac{2e}{\hbar} \int \frac{d\omega}{2\pi} n_F(\omega) \sum_{\mathbf{k}nm} \text{Tr} \left\{ \text{Re} \left[ m^3 G_{d,nm}^R(\omega) M_{\text{hyb}}^{(\alpha m)\dagger} g_{\mathbf{k}\alpha}^R(\omega) M_{\text{hyb}}^{(\alpha n)} - m^3 G_{d,nm}^A(\omega) M_{\text{hyb}}^{(\alpha m)\dagger} g_{\mathbf{k}\alpha}^A(\omega) M_{\text{hyb}}^{(\alpha n)} \right] \right\}. \quad (4.95)$$

Here, we used the cyclic property of the trace. Thus, we can identify the self-energy for lead  $\alpha$  here, which is for the retarded or advanced functions

$$\Sigma_{d,mn}^{R/A(\alpha)}(\omega) = M_{\text{hyb}}^{(\alpha m)\dagger} g_{\mathbf{k}\alpha}^{R/A}(\omega) M_{\text{hyb}}^{(\alpha n)}. \quad (4.96)$$

We already found these for the imaginary time formalism, Eq. (4.57), and they can be obtained for real times via analytic continuation. The current thus becomes

$$\begin{aligned} J_\alpha &= -\frac{2e}{\hbar} \int \frac{d\omega}{2\pi} n_F(\omega) \sum_{nm} \text{Tr} \left\{ \text{Re} \left[ m^3 G_{d,nm}^R(\omega) \Sigma_{d,mn}^{R(\alpha)}(\omega) - m^3 G_{d,nm}^A(\omega) \Sigma_{d,mn}^{A(\alpha)}(\omega) \right] \right\} \\ &= -\frac{2e}{\hbar} \int \frac{d\omega}{2\pi} n_F(\omega) \text{Tr} \left\{ \text{Re} \left[ m^3 \text{Tr}_d \left\{ G_d^R(\omega) \Sigma_d^{R(\alpha)}(\omega) - G_d^A(\omega) \Sigma_d^{A(\alpha)}(\omega) \right\} \right] \right\}. \end{aligned} \quad (4.97)$$

In the second line we expressed the Green function and self-energy as matrices in the dot level space, where the trace  $\text{Tr}_d$  runs now over the dot levels and  $\text{Tr}$  is still the trace in the Nambu space.

## 4.4 The one-level dot system

We will now consider a special case of our system, i.e., the dot consists of only one energy level which couples to a left and right superconducting lead. We will determine the spectral function as defined in Eq. (3.72), first for the uncoupled parts, then for the total system. Thus, we can find the Andreev bound states. We will also investigate how the bound states depend on other parameters such as the phase difference or the coupling strength. Then we would like to see what happens when we add a third, normal lead, which we can do in principle, since the Green functions we determined have been independent of the number of leads so far. After that we will determine the current.

We measure energies in units of our gap  $\Delta$  and assume a low temperature of the order of  $10^{-3}\Delta$ . This corresponds to cryostat temperatures for gap sizes of standard materials like aluminum or lead [12].

### 4.4.1 Spectral function and Andreev bound states

Let us have a look at first at the spectral function for the unperturbed (uncoupled) lead  $\alpha$ . The spectral function is here calculated as

$$A_{\alpha}^0(\omega) = \sum_{\mathbf{k}} i (g_{\mathbf{k}\alpha}^R(\omega) - g_{\mathbf{k}\alpha}^A(\omega)). \quad (4.98)$$

The Green functions for the free leads have already been determined in the imaginary time formalism in Eq. (4.29). Thus, the retarded and advanced functions can be determined by analytic continuation. We sum here over  $\mathbf{k}$ , because we want to determine the spectral function independent of  $\mathbf{k}$ . This sum has been done already in Eq. (4.54). Since the spectral function is of a  $(2 \times 2)$ -matrix form, we plotted the diagonal terms for different gap energies in Fig. 6, and the off-diagonal terms are shown in Fig. 7. Thereby, it is  $A_{\alpha;11}^0(\omega) = A_{\alpha;22}^0(\omega)$  and  $A_{\alpha;12}^0(\omega) = A_{\alpha;21}^0(\omega)$ . We see for the diagonal elements the typical spectral density for a superconductor with an energy gap between  $-\Delta_{\alpha}$  and  $+\Delta_{\alpha}$ . The off-diagonal elements have negative parts, which is atypical for the spectral function.

Next, we would like to determine the spectral function for the uncoupled dot,

$$A_{d,11}^0(\omega) = i (g_{d,11}^R(\omega) - g_{d,11}^A(\omega)), \quad (4.99)$$

which we wrote here with the dot indices.

The free dot Matsubara Green function for the  $m$ -th level for noninteracting electrons has been determined in Eq. (4.45). After analytic continuation we can use the theorem Eq. (3.74). Thus, in the limit of  $\eta \rightarrow 0^+$ , we obtain as expected a diagonal spectral function that contains delta functions,

$$A_{d,11}^0(\omega) = 2\pi \begin{pmatrix} \delta(\omega - \xi_{d1}) & 0 \\ 0 & \delta(\omega + \xi_{d1}) \end{pmatrix}. \quad (4.100)$$

Fig. 8 shows the spectral function for finite broadening, i.e., finite  $\eta$ . The diagonal elements of the spectral function are symmetric due to particle-hole symmetry. Now we are going to show how the spectral function for the dot changes when we couple it with the leads. The spectral function for the coupled dot is,

$$A_{d,11}(\omega) = i (G_{d,11}^R(\omega) - G_{d,11}^A(\omega)). \quad (4.101)$$

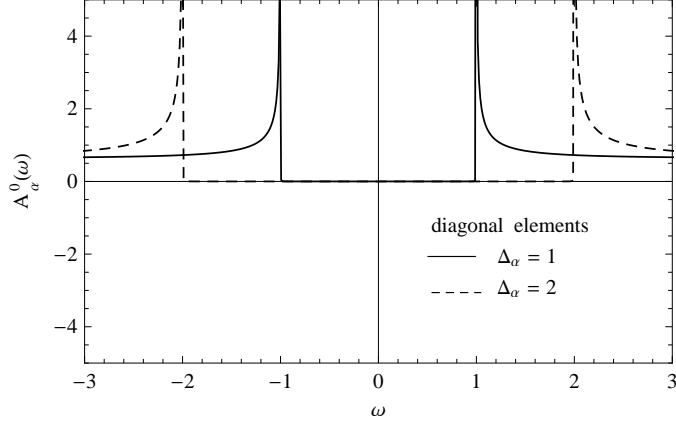


**Figure 6:** Diagonal elements of the spectral function for lead  $\alpha$  for different gap energies, with the constant density of states  $\nu_F^\alpha = 0.1$ , and finite  $\eta = 10^{-4}$ . The diagonal elements are equal, that is why there is only one plot for each gap energy. The spectral function shows the typical energy resolution of a superconductor, with an energy gap between  $-\Delta_\alpha$  and  $+\Delta_\alpha$ . It also shows the particle-hole symmetry that we implied with the Nambu representation.

In Eq. (4.52) we found the Matsubara dot Green function for the total system. For the case of one level, this is now a  $(2 \times 2)$ -matrix. Let us have a look at the retarded dot Green function at first, that we get from analytic continuation of the inversion of Eq. (4.52),

$$G_{d,11}^R(\omega) = \left( g_{d,11}^R(\omega)^{-1} - \Sigma_{d,11}^R(\omega) \right)^{-1}. \quad (4.102)$$

In Eq. (4.53) we obtained the  $(mn)$ -matrix element of the Matsubara dot Green function of the unperturbed system. After analytic continuation we get for the one level retarded dot Green function,

$$g_{d,11}^R(\omega) = \begin{pmatrix} \frac{1}{\omega + i\eta - \xi_{d1\uparrow}} & 0 \\ 0 & \frac{1}{\omega + i\eta + \xi_{d1\downarrow}} \end{pmatrix}. \quad (4.103)$$

The corresponding self-energy is obtained through analytic continuation of Eq. (4.57). It follows then,

$$\Sigma_{d,11}^R(\omega) = \sum_{\alpha} \Sigma_{d,11}^{R(\alpha)}(\omega) \quad (4.104)$$

$$= - \sum_{\alpha} \frac{\pi \nu_F^\alpha}{E_\alpha(\omega + i\eta)} \begin{pmatrix} |t_{\alpha 1}|^2(\omega + i\eta) & (t_{\alpha 1}^2)^* \Delta_\alpha \\ t_{\alpha 1}^2 \Delta_\alpha^* & |t_{\alpha 1}|^2(\omega + i\eta) \end{pmatrix}. \quad (4.105)$$

Therefore, we obtain

$$G_{d,11}^R(\omega) = \frac{1}{D_{11}(\omega + i\eta)} \left[ \begin{pmatrix} \omega + i\eta + \xi_{d1\downarrow} & 0 \\ 0 & \omega + i\eta - \xi_{d1\uparrow} \end{pmatrix} + \sum_{\alpha} \frac{\pi \nu_F^\alpha}{E_\alpha(\omega + i\eta)} \begin{pmatrix} |t_{\alpha 1}|^2(\omega + i\eta) & -(t_{\alpha 1}^2)^* \Delta_\alpha \\ -t_{\alpha 1}^2 \Delta_\alpha^* & |t_{\alpha 1}|^2(\omega + i\eta) \end{pmatrix} \right], \quad (4.106)$$

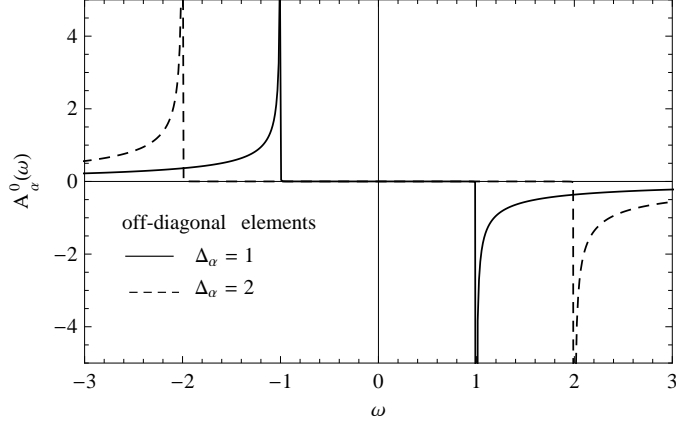


**Figure 7:** Off-diagonal elements of the spectral function for lead  $\alpha$  for different gap energies, with  $\nu_F^\alpha = 0.1$ ,  $\eta = 10^{-4}$ . The off-diagonal matrix entries are equal for each gap energy. Here, the off-diagonal elements of the spectral function become negative on the positive axis, which is atypical for spectral functions.

where we defined the determinant of the Green function

$$D_{11}(\omega + i\eta) = \det [G_{d,11}^R(\omega)^{-1}] \quad (4.107)$$

$$\begin{aligned} &= \left[ \omega + i\eta - \xi_{d1\uparrow} + \pi(\omega + i\eta) \sum_{\alpha} \frac{\nu_F^\alpha |t_{\alpha 1}|^2}{E_{\alpha}(\omega + i\eta)} \right] \\ &\quad \times \left[ \omega + i\eta + \xi_{d1\downarrow} + \pi(\omega + i\eta) \sum_{\alpha} \frac{\nu_F^\alpha |t_{\alpha 1}|^2}{E_{\alpha}(\omega + i\eta)} \right] \\ &\quad - \sum_{\alpha\alpha'} \frac{\pi^2 \nu_F^\alpha \nu_F^{\alpha'} (t_{\alpha 1} t_{\alpha' 1}^*)^2 \Delta_{\alpha'} \Delta_{\alpha}^*}{E_{\alpha}(\omega + i\eta) E_{\alpha'}(\omega + i\eta)}. \end{aligned} \quad (4.108)$$

We are going to do some simplifications here. The gap energies of the leads shall have the same amplitude, but different phases, i.e.,  $\Delta_{\alpha} = |\Delta| e^{i\phi_{\alpha}}$ . Therefore, it is  $E_{\alpha}(\omega + i\eta) = E(\omega + i\eta) = \sqrt{|\Delta|^2 - (\omega + i\eta)^2}$ . We can introduce a phase for the coupling terms as well,  $t_{\alpha m} = |t_{\alpha m}| e^{i\theta_{\alpha m}}$ . Furthermore, we would like to use the definition of a quantity that gives the transition rate between lead  $\alpha$  and dot,

$$\Gamma_{\alpha 1} = 2\pi \nu_F^\alpha |t_{\alpha 1}|^2, \quad (4.109)$$

where the total transition rate is then  $\Gamma = \Gamma_{l1} + \Gamma_{r1}$ . Thus Eq. (4.106) modifies to

$$\begin{aligned} G_{d,11}^R(\omega) &= \frac{1}{D_{11}(\omega + i\eta)} \left[ \begin{pmatrix} \omega + i\eta + \xi_{d1\downarrow} & 0 \\ 0 & \omega + i\eta - \xi_{d1\uparrow} \end{pmatrix} \right. \\ &\quad \left. + \frac{1}{2} \sum_{\alpha} \frac{\Gamma_{\alpha 1}}{E(\omega + i\eta)} \begin{pmatrix} \omega + i\eta & -|\Delta| e^{i\varphi_{\alpha}} \\ -|\Delta| e^{-i\varphi_{\alpha}} & \omega + i\eta \end{pmatrix} \right], \end{aligned} \quad (4.110)$$

where we put  $\varphi_{\alpha} = \phi_{\alpha} - 2\theta_{\alpha 1}$ . Furthermore, the self-energy becomes

$$\Sigma_{d,11}^R(\omega) = -\frac{1}{2} \sum_{\alpha} \frac{\Gamma_{\alpha 1}}{E(\omega + i\eta)} \begin{pmatrix} \omega + i\eta & |\Delta| e^{i\varphi_{\alpha}} \\ |\Delta| e^{-i\varphi_{\alpha}} & \omega + i\eta \end{pmatrix}. \quad (4.111)$$

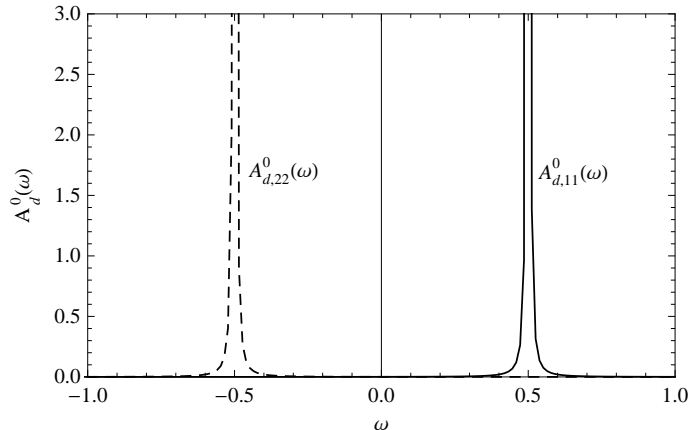


**Figure 8:** The free dot spectral function for noninteracting electrons for finite  $\eta = 10^{-4}$ . The dot level is at  $\xi_{d1} = 0.5$ . The diagonal elements are symmetric due to particle-hole symmetry. Off-diagonal elements are zero.

For the determinant we get

$$D_{11}(\omega + i\eta) = \left[ \omega + i\eta - \xi_{d1\uparrow} + \frac{(\omega + i\eta)\Gamma}{2E(\omega + i\eta)} \right] \left[ \omega + i\eta + \xi_{d1\downarrow} + \frac{(\omega + i\eta)\Gamma}{2E(\omega + i\eta)} \right] - \frac{|\Delta|^2}{4E(\omega + i\eta)^2} \underbrace{[\Gamma_{l1}^2 + \Gamma_{r1}^2 + 2\Gamma_{l1}\Gamma_{r1} \cos(\delta\phi)]}_{\Gamma^2 - 4\Gamma_{l1}\Gamma_{r1} \sin^2(\frac{\delta\phi}{2})}, \quad (4.112)$$

where  $\delta\phi = \varphi_r - \varphi_l = \phi_r - \phi_l - 2(\theta_{r1} - \theta_{l1})$  is the phase difference that contains the phases for the leads as well as the coupling terms. Those phases are adjusted by application of a bias voltage or magnetic fields. Thereby, only the phase difference is really measurable.

The advanced Green function can simply be found by the hermitian conjugate of the retarded Green function. Thus, we are now able to calculate the spectral function for the dot,

$$A_{d,11}(\omega) = i \left( G_{d,11}^R(\omega) - G_{d,11}^{R\dagger}(\omega) \right). \quad (4.113)$$

Fig. 9 shows the four matrix elements of the spectral function, where energies like the dot level or the coupling strength are in units of  $|\Delta|$  which we just write as  $\Delta$ . Thereby, the off-diagonal elements become negative again and they further have an imaginary part. For a low dot level, compared to  $\Delta$ , we find two clear peaks in the superconducting gap in a) - c), which can be interpreted as the particle-hole symmetric Andreev bound states. They are to be found at a different energy than the dot level, i.e., the bound states are  $\omega_b \approx 0.28\Delta$  for a dot level of  $\xi_{d1} = 0.1\Delta$  with the gap parameter  $|\Delta| = 1$ . In d) we show the spectral function for the case we move the dot level much higher than the gap energy. Thereby, the bound state approaches the gap energy and additionally there appears a peak in the continuum part of the spectral function at the dot energy, which is in accordance with [13].

Another way of finding the bound states is to check where the determinant Eq. (4.112) becomes zero, since it is in the denominator of the Green function Eq. (4.110). Therefore, the spectral function blows up, where the determinant is zero, which happens exactly at the bound states. Fig. 10 shows the zeros of the determinant for different parameter dependencies. We find the bound states vs. dot level relations to be in accordance with [14].

We can find an analytic expression for the bound states in terms of an asymptotic approach. Therefore we set the determinant, Eq. (4.112), zero. Then we multiply the equation with the energy  $E(\omega + i\eta)^2 = |\Delta|^2 - (\omega + i\eta)$  and take as well the limit  $\eta \rightarrow 0^+$ . This gives,

$$0 = (|\Delta|^2 - \omega_b^2)(\omega_b^2 - \xi_{d1}^2 - \frac{1}{4}\Gamma^2) + \Gamma_{l1}\Gamma_{r1}|\Delta|^2 \sin^2\left(\frac{\delta\phi}{2}\right) + \Gamma\omega_b^2\sqrt{|\Delta|^2 - \omega_b^2}. \quad (4.114)$$

We would like to express this in terms of the Breit-Wigner transmission probability at the Fermi level [6],

$$T_{\text{BW}} = \frac{\Gamma_{l1}\Gamma_{r1}}{\xi_{d1}^2 + \frac{1}{4}\Gamma^2}. \quad (4.115)$$

Thus, we obtain

$$\omega_b^2 = |\Delta|^2 \frac{\xi_{d1}^2 + \frac{1}{4}\Gamma^2}{\xi_{d1}^2 + \left(\sqrt{|\Delta|^2 - \omega_b^2} + \frac{1}{2}\Gamma\right)^2} \left[1 - T_{\text{BW}} \sin^2\left(\frac{\delta\phi}{2}\right)\right]. \quad (4.116)$$

In the limit of  $|\Delta^2 - \omega_b^2| \ll \Gamma^2/4$ , we get

$$\omega_b^2 = |\Delta|^2 \left[1 - T_{\text{BW}} \sin^2\left(\frac{\delta\phi}{2}\right)\right]. \quad (4.117)$$

This is found as well in [15], where they study the short-junction limit of a Josephson junction, i.e., the junction between two superconductors is assumed to be small compared to the superconducting coherence length, which corresponds to our case as well.

We would like to see how the spectral function changes when we add an additional, normal lead to our system. We can simply include the third lead in the Green function, Eq. (4.110), respectively the determinant, Eq. (4.112), as they are still of the form for a general number of leads. The normal lead is then coupled with the strength  $\Gamma_{N1}$  and the energy gap for this lead is zero, of course. Fig. 11 shows the (11)-component of the spectral function for this system. We find, that the spectrum between the gap energies broadens, which is consistent with [16]. Thereby, the broadening is more pronounced the stronger the normal lead is coupled.

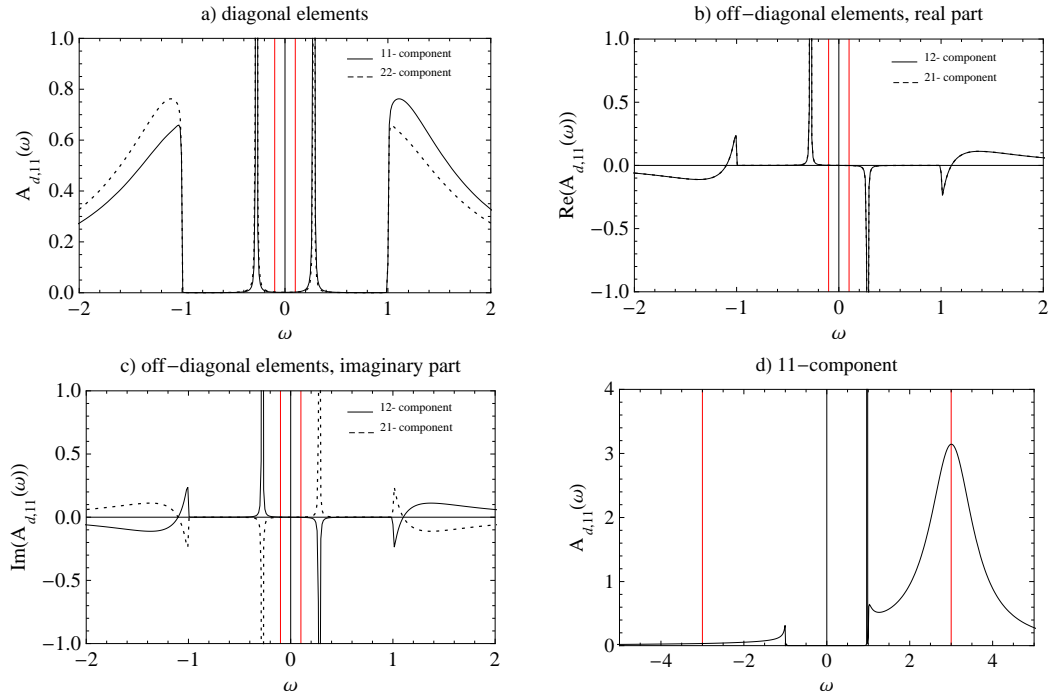


**Figure 9:** Spectral function for the dot coupled to the two superconducting reservoirs. The plots a) - c) show diagonal and off-diagonal elements separately. Thereby, the off-diagonal elements have an imaginary part as well. The dot level energy is marked in the plots with a red line. For a) -c) it is at  $\xi_{d1} = 0.1\Delta$ . Further parameters are  $|\Delta| = 1$ ,  $\Gamma_{l1} = \Gamma_{r1} = 0.6\Delta$ ,  $\varphi_r = \pi/2$ ,  $\varphi_l = 0$ ,  $\eta = 10^{-4}$ . The bound states are to be found at  $\omega_b \approx 0.28\Delta$ . In d) we show the (11)-component of the spectral function for the same parameters but for a dot level at  $\xi_{d1} = 3\Delta$ .

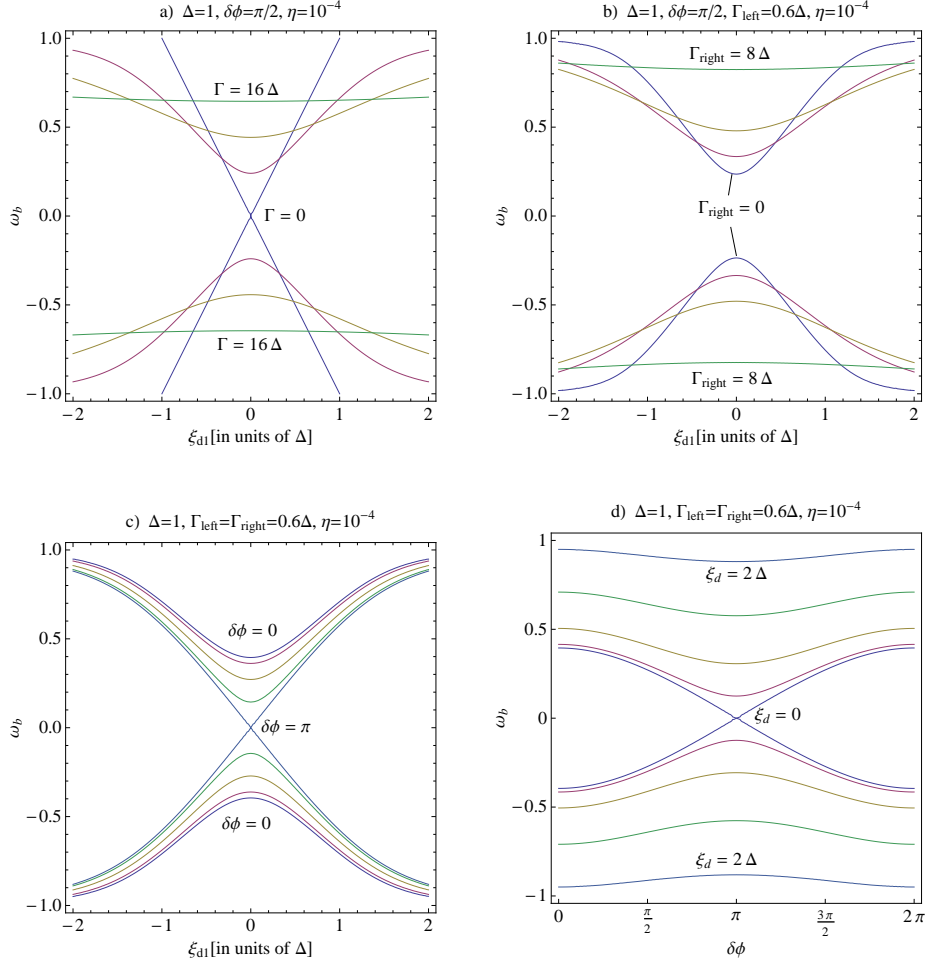


**Figure 10:** The plots show how the bound states depend on several parameters. They are made as a contour plot by showing only those parts where the determinant becomes zero, which happens exactly at the bound states called  $\omega_b$ . Plot a) shows the bound states with respect to the dot level energy for different coupling strengths  $\Gamma = \Gamma_{\text{left}} + \Gamma_{\text{right}}$ . If dot and leads are decoupled,  $\Gamma = 0$ , we get the linear relation we already found for the spectrum of the free dot. For high coupling strengths the bound states become independent of the dot level. In b) we vary the coupling strength on the right side while keeping the left one constant. For  $\Gamma_{\text{right}} = 0$  we show the case for the dot being coupled to only one lead. If we increase  $\Gamma_{\text{right}}$  the bound states become again independent of the dot level energy. c) shows the bound states with respect to the dot level energy for different phase differences. At  $\delta\phi = \pi$  the relation between bound states and dot level approaches a linear behavior, like in a) for  $\Gamma = 0$ , which suggests a decoupling of dot and leads. In d) we show the bound states with respect to the phase difference for different dot levels. All plots show that if we increase the dot level energies, the bound states approach the gap energies.

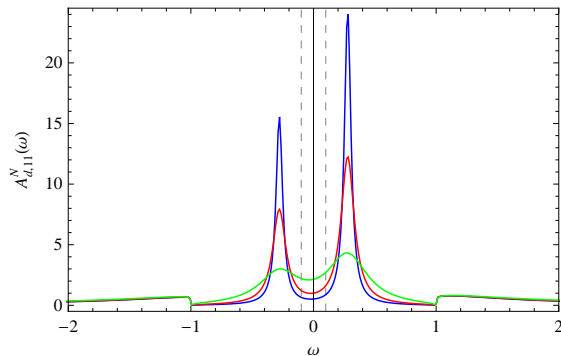


**Figure 11:** Spectral function for the addition of a normal lead. The plot shows the energy gap region of the (11)-component of the spectral function, where  $|\Delta| = 1$  again. The dot level is at  $\xi_{d1} = 0.1\Delta$  (dashed lines). Further parameters are  $\Gamma_{l1} = \Gamma_{r1} = 0.6\Delta$ ,  $\varphi_r = \pi/2$ ,  $\varphi_l = 0$ . The normal lead causes a broadening of the sub-gap spectrum. Thereby, the broadening is more pronounced for higher coupling parameters,  $\Gamma_{N1} = 0.1\Delta$  (blue),  $0.2\Delta$  (red),  $0.6\Delta$  (green). The broadening caused by  $\eta$  is negligible here.

#### 4.4.2 The current

We would like to determine the current for our 1-level dot system. The current formula has been derived for a general number of level in Eq. (4.97) and looks in our case now as follows,

$$\begin{aligned} J_\alpha^{(1)} &= -\frac{2e}{\hbar} \int \frac{d\omega}{2\pi} n_F(\omega) \text{Tr} \left\{ \text{Re} \left[ m^3 G_{d,11}^R(\omega) \Sigma_{d,11}^{R(\alpha)}(\omega) - m^3 G_{d,11}^A(\omega) \Sigma_{d,11}^{A(\alpha)}(\omega) \right] \right\} \\ &= -\frac{2e}{\hbar} \int \frac{d\omega}{2\pi} n_F(\omega) \text{Tr} \left\{ \text{Re} \left[ m^3 G_{d,11}^R(\omega) \Sigma_{d,11}^{R(\alpha)}(\omega) - m^3 G_{d,11}^{R\dagger}(\omega) \Sigma_{d,11}^{R(\alpha)\dagger}(\omega) \right] \right\}, \end{aligned} \quad (4.118)$$

where we used the fact that the self-energy of the advanced Green function can also be obtained by hermitian conjugation of the self-energy for the retarded Green function.

If we take the trace over the Nambu space and take the real part, we get another real part,

$$J_\alpha^{(1)} = -\frac{2e}{\hbar} \int \frac{d\omega}{2\pi} n_F(\omega) 2\text{Re} \left[ G_{d,11;12}^R(\omega) \Sigma_{d,11;21}^{R(\alpha)}(\omega) - G_{d,11;21}^R(\omega) \Sigma_{d,11;12}^{R(\alpha)}(\omega) \right], \quad (4.119)$$

which we wrote with Nambu indices now. Now, we use the fact, that we can write the Green function in terms of the self energy. Compare Eqs. (4.110) and (4.111), then we can write

$$G_{d,11;12}^R(\omega) = \frac{1}{D_{11}(\omega + i\eta)} \Sigma_{d,11;12}^R(\omega) = \frac{1}{D_{11}(\omega + i\eta)} \left[ \Sigma_{d,11;12}^{R(\alpha)}(\omega) + \Sigma_{d,11;12}^{R(\bar{\alpha})}(\omega) \right], \quad (4.120)$$

$$G_{d,11;21}^R(\omega) = \frac{1}{D_{11}(\omega + i\eta)} \Sigma_{d,11;21}^R(\omega) = \frac{1}{D_{11}(\omega + i\eta)} \left[ \Sigma_{d,11;21}^{R(\alpha)}(\omega) + \Sigma_{d,11;21}^{R(\bar{\alpha})}(\omega) \right], \quad (4.121)$$

where  $\bar{\alpha} = r$  if  $\alpha = l$  or the other way around. The labels  $l$  and  $r$  stand for the left and right lead. Accordingly, the current formula reduces to

$$J_\alpha^{(1)} = -\frac{2e}{\hbar} \int \frac{d\omega}{2\pi} n_F(\omega) 2\text{Re} \left\{ \frac{1}{D_{11}(\omega + i\eta)} \left[ \Sigma_{d,11;12}^{R(\bar{\alpha})}(\omega) \Sigma_{d,11;21}^{R(\alpha)}(\omega) - \Sigma_{d,11;21}^{R(\bar{\alpha})}(\omega) \Sigma_{d,11;12}^{R(\alpha)}(\omega) \right] \right\}. \quad (4.122)$$

As we see,  $J_\alpha^{(1)} = -J_{\bar{\alpha}}^{(1)}$ . That means, if we calculate the total current as  $J^{(1)} = \frac{1}{2}(J_l^{(1)} - J_r^{(1)})$ , it is  $J^{(1)} = J_l^{(1)} = -J_r^{(1)}$ . Therefore, we obtain for the total current

$$J^{(1)} = -\frac{2e}{\hbar} \int \frac{d\omega}{2\pi} n_F(\omega) 2\text{Re} \left\{ \frac{1}{D_{11}(\omega + i\eta)} \left[ \Sigma_{d,11;12}^{R(r)}(\omega) \Sigma_{d,11;21}^{R(l)}(\omega) - \Sigma_{d,11;21}^{R(r)}(\omega) \Sigma_{d,11;12}^{R(l)}(\omega) \right] \right\}. \quad (4.123)$$

The self-energies can be taken from Eq. (4.111),

$$\Sigma_{d,11;12}^{R(\alpha)}(\omega) = -\frac{|\Delta| \Gamma_{\alpha 1} e^{i\varphi_\alpha}}{2E(\omega + i\eta)}, \quad (4.124)$$

$$\Sigma_{d,11;21}^{R(\alpha)}(\omega) = -\frac{|\Delta| \Gamma_{\alpha 1} e^{-i\varphi_\alpha}}{2E(\omega + i\eta)}. \quad (4.125)$$

This gives

$$J^{(1)} = \frac{2e}{\hbar} \Gamma_{l1} \Gamma_{r1} |\Delta|^2 \sin(\delta\phi) \int \frac{d\omega}{2\pi} n_F(\omega) \text{Im} \left[ \frac{1}{D_{11}(\omega + i\eta) E(\omega + i\eta)^2} \right], \quad (4.126)$$

where we used, that for a complex number  $z$  it is  $\text{Re}[iz] = -\text{Im}[z]$ .

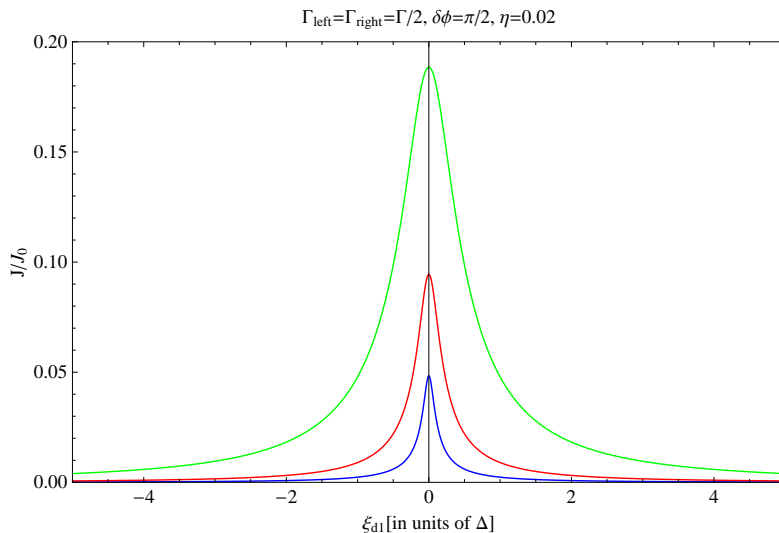


**Figure 12:** Supercurrent vs. dot level energy for different gap energies. The current has its maximum at  $\xi_{d1} = 0$  and decays towards zero if the dot level is shifted up or down. The maximum depends on the coupling strength. Here we show the cases  $\Gamma = 0.2\Delta$  (blue),  $0.4\Delta$  (red),  $1\Delta$  (green).

The expression in the integrand, which is the product of the determinant, Eq. (4.112), and the square of the energy we defined as  $E(\omega + i\eta) = \sqrt{|\Delta|^2 - (\omega + i\eta)^2}$ , looks as follows,

$$\begin{aligned}
 D_{11}(\omega + i\eta)E(\omega + i\eta)^2 = & \left[ (\omega + i\eta - \xi_{d1\uparrow})\sqrt{|\Delta|^2 - (\omega + i\eta)^2} + \frac{1}{2}(\omega + i\eta)\Gamma \right] \\
 & \times \left[ (\omega + i\eta + \xi_{d1\downarrow})\sqrt{|\Delta|^2 - (\omega + i\eta)^2} + \frac{1}{2}(\omega + i\eta)\Gamma \right] \\
 & - \frac{1}{4}|\Delta|^2 \left[ \Gamma^2 - 4\Gamma_{l1}\Gamma_{r1} \sin^2 \left( \frac{\delta\phi}{2} \right) \right]. \quad (4.127)
 \end{aligned}$$

We are now able to calculate the current numerically. For the following plots we had to choose finite  $\eta$ , otherwise numerical errors occurred, but we tried to make them as small as possible. Since the electrons in the dot are noninteracting, it is  $\xi_{d1\uparrow} = \xi_{d1\downarrow} = \xi_{d1}$ . Furthermore, we assume equal coupling strengths on both sides, i.e.,  $\Gamma_{l1} = \Gamma_{r1} = \Gamma/2$ .

In Fig. 12 we show the supercurrent vs. the dot level energy for different coupling strengths. Thereby, we show the current in units of  $J_0 = e\Delta/\hbar$ . We find it to be in accordance with [14]. We see that the current is maximal for  $\xi_{d1} = 0$ , whereas stronger coupling means higher maxima. If we shift the level up or down, the current decreases towards zero.

In Fig. 13 we compare the supercurrent to the coupling strength  $\Gamma = \Gamma_{l1} + \Gamma_{r1}$  for different dot level. The current is zero for  $\Gamma = 0$  for all dot level, which is exactly the case when dot and lead are decoupled. For  $\Gamma \neq 0$ , the current is higher the closer the dot level is to zero. If the coupling is further increased, the current approaches an asymptotic value independent of the dot level.

Fig. 14 shows the dependence of the supercurrent on the phase difference for different coupling strengths. The current is  $2\pi$ -periodic as the result of the current, Eq. (4.126), suggests. We have already found that lead and dot decouple for a phase difference of  $\delta\phi = \pi$ , Fig. 10 c). This means that the current must vanish in this case, which we found here as well. The maximum current is found at different  $\delta\phi$  for different  $\Gamma$ .

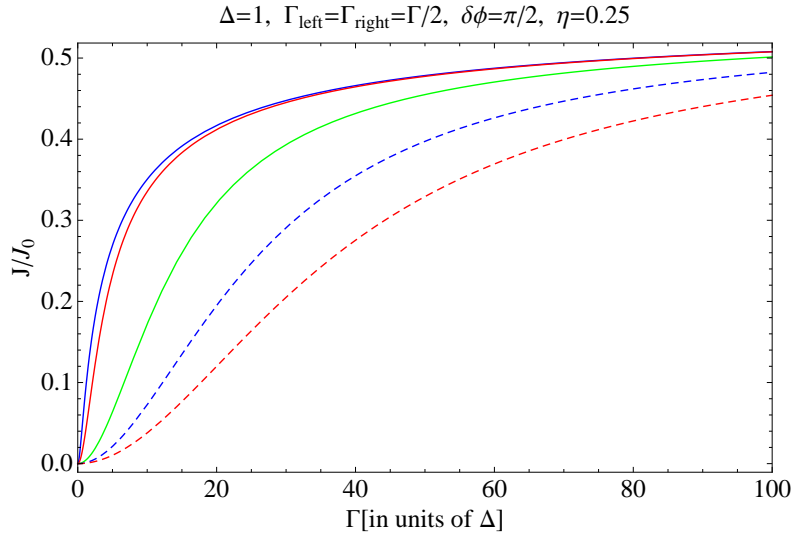


**Figure 13:** Supercurrent vs. coupling strength for different dot levels. From the solid blue to the dashed red curve it is  $\xi_{d1} = 0, 1, 2, 5, 10, 15\Delta$ . It is  $\Gamma = \Gamma_{l1} + \Gamma_{r1}$ . The current starts at zero for  $\Gamma = 0$  for all level energies. For an increasing coupling strength the current increases and approaches an asymptote. In the beginning, the current is strongest for the dot level at zero energy, whereas the asymptotic value is independent of the dot level.

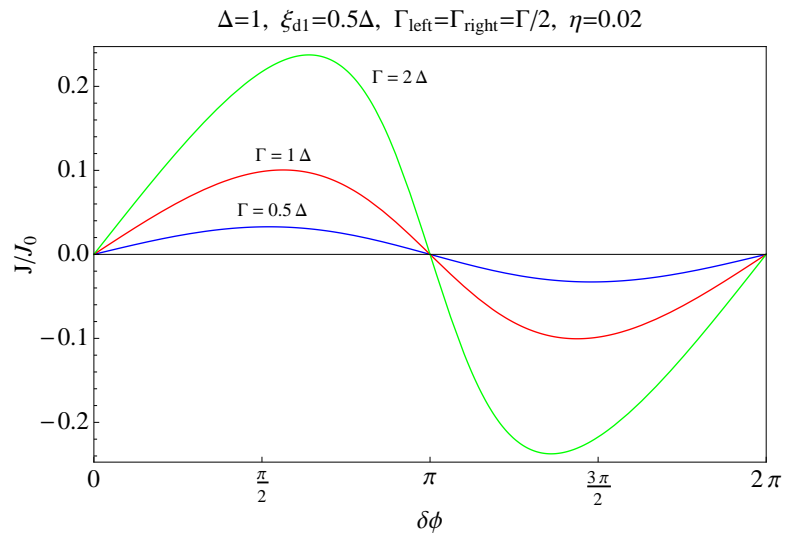


**Figure 14:** Supercurrent vs. phase difference for different coupling strengths.

## Comparison to Beenakker and van Houten

We would like to compare our result for the current to the one in [6], where the system is treated by means of a scattering formalism.

First of all we rewrite the expression Eq. (4.127) with  $\xi_{d1\uparrow} = \xi_{d1\downarrow} = \xi_{d1}$  and rename it as follows,

$$\begin{aligned} B(\omega + i\eta) &= D_{11}(\omega + i\eta)E(\omega + i\eta)^2 \\ &= \left(|\Delta|^2 - (\omega + i\eta)^2\right) \left((\omega + i\eta)^2 - \xi_{d1}^2 - \frac{1}{4}\Gamma^2\right) + |\Delta|^2\Gamma_{l1}\Gamma_{r1} \sin^2\left(\frac{\delta\phi}{2}\right) \\ &\quad + \Gamma(\omega + i\eta)^2 \left(|\Delta|^2 - (\omega + i\eta)^2\right)^{1/2}, \end{aligned} \quad (4.128)$$

with  $\Gamma = \Gamma_{l1} + \Gamma_{r1}$ . The current is then

$$J^{(1)} = \frac{2e}{\hbar}\Gamma_{l1}\Gamma_{r1}|\Delta|^2 \sin(\delta\phi) \int \frac{d\omega}{2\pi} n_F(\omega) \text{Im} \left[ \frac{1}{B(\omega + i\eta)} \right]. \quad (4.129)$$

We split the current into two parts,

$$J^{(1)} = J_{\Delta}^{(1)} + J_{\infty}^{(1)}, \quad (4.130)$$

where  $J_{\Delta}^{(1)}$  contains the integral part with frequencies between the gaps and  $J_{\infty}^{(1)}$  is for the continuous spectrum outside the gap.

Let us calculate  $J_{\Delta}^{(1)}$  first,

$$J_{\Delta}^{(1)} = \frac{2e}{\hbar}\Gamma_{l1}\Gamma_{r1}|\Delta|^2 \sin(\delta\phi) \int_{-\Delta}^{\Delta} \frac{d\omega}{2\pi} n_F(\omega) \text{Im} \left[ \frac{1}{B(\omega + i\eta)} \right]. \quad (4.131)$$

We can expand  $B(\omega + i\eta)$  around  $\omega$ , which gives  $B(\omega + i\eta) \simeq B(\omega) + i\eta B'(\omega)$ . We will use the fact that  $B(\omega)$  and  $B'(\omega)$  are real numbers, because for  $J_{\Delta}^{(1)}$  we have only the contribution for  $\omega^2 < |\Delta|^2$ . Then, we get for the imaginary part in the integral

$$\begin{aligned} \text{Im} \left[ \frac{1}{B(\omega + i\eta)} \right] &= \text{Im} \left[ \frac{1}{B(\omega) + i\eta B'(\omega)} \right] \\ &= \frac{1}{B'(\omega)} \text{Im} \left[ \frac{1}{B(\omega)B'(\omega)^{-1} + i\eta} \right], \quad \text{use Eq. (3.74)} \\ &= -\frac{\pi}{B'(\omega)} \delta(B(\omega)B'(\omega)^{-1}) \\ &= -\frac{\pi}{B'(\omega)} \sum_i \frac{\delta(\omega - \varepsilon_i)}{|h'(\varepsilon_i)|}. \end{aligned} \quad (4.132)$$

Here, we defined  $h(\omega) = B(\omega)B'(\omega)^{-1}$ . Then we used the fact, that if the delta function has another function  $f(x)$  as an argument, it can be expressed the following way,

$$\delta(f(x)) = \sum_i \frac{\delta(x - x_i)}{|f'(x_i)|}, \quad (4.133)$$

where the sum is over all roots of  $f(x)$ . The roots of  $h(\omega)$  are called  $\varepsilon_i$  here, and moreover they correspond to the Andreev bound states. Furthermore, it is  $h(\varepsilon_i) = 0$  as  $B(\varepsilon_i) \stackrel{!}{=} 0$ , therefore it turns out that  $h'(\varepsilon_i) = 1$ . Thus, we obtain

$$\text{Im} \left[ \frac{1}{B(\omega + i\eta)} \right] = -\pi \sum_i \frac{\delta(\omega - \varepsilon_i)}{B'(\omega)} \quad (4.134)$$

$$= -\pi \sum_i \frac{\delta(\omega - \varepsilon_i)}{B'(\varepsilon_i)}, \quad (4.135)$$

where we could replace the argument in  $B'(\omega)$  by  $\varepsilon_i$ , because of the delta function. We now use the fact, that the bound states are a function of the phase difference,  $\varepsilon_i = \varepsilon_i(\delta\phi)$ . We have seen that in the discussion above, see also Fig. 10 d). Therefore, it is  $B(\varepsilon_i) = B(\varepsilon_i(\delta\phi), \delta\phi) = 0$  and thus

$$\frac{d}{d\delta\phi} B(\varepsilon_i(\delta\phi), \delta\phi) = \frac{\partial B}{\partial \varepsilon_i} \frac{\partial \varepsilon_i}{\partial \delta\phi} + \frac{\partial B}{\partial \delta\phi} = 0. \quad (4.136)$$

So we obtain an expression for  $B'(\varepsilon_i) = \partial B / \partial \varepsilon_i$ ,

$$\begin{aligned} B'(\varepsilon_i) &= -\frac{\partial B}{\partial \delta\phi} \left( \frac{\partial \varepsilon_i}{\partial \delta\phi} \right)^{-1} \\ &= -\frac{1}{2} \Gamma_{l1} \Gamma_{r1} |\Delta|^2 \sin(\delta\phi) \left( \frac{\partial \varepsilon_i}{\partial \delta\phi} \right)^{-1}, \end{aligned} \quad (4.137)$$

where we calculated the derivative with respect to  $\delta\phi$  by using the definition of  $B(\omega)$ , Eq. (4.128). The result for  $B'(\varepsilon_i)$  can be plugged into Eq. (4.135), and this can be used for the current in Eq. (4.131). Thus, we obtain

$$\begin{aligned} J_{\Delta}^{(1)} &= \frac{2e}{\hbar} \sum_i \int_{-\Delta}^{\Delta} d\omega n_F(\omega) \delta(\omega - \varepsilon_i) \frac{\partial \varepsilon_i}{\partial \delta\phi} \\ &= \frac{2e}{\hbar} \sum_i n_F(\varepsilon_i) \frac{\partial \varepsilon_i}{\partial \delta\phi} \\ &= \frac{2e}{\hbar} \sum_{\varepsilon_i > 0} [n_F(\varepsilon_i) - n_F(-\varepsilon_i)] \frac{\partial \varepsilon_i}{\partial \delta\phi} \\ &= -\frac{2e}{\hbar} \sum_{\varepsilon_i > 0} \tanh\left(\frac{\varepsilon_i}{2k_B T}\right) \frac{\partial \varepsilon_i}{\partial \delta\phi}. \end{aligned} \quad (4.138)$$

Because of the particle-hole symmetry, the bound states always come in pairs of  $\pm\varepsilon_i$ . We used this fact to rewrite the sum. Then we can identify the hyperbolic tangent from the difference of the Fermi functions.

We would like to calculate the rest of the current now, i.e., the part with the contributions from the continuous spectrum,

$$J_{\infty}^{(1)} = \frac{2e}{\hbar} \Gamma_{l1} \Gamma_{r1} |\Delta|^2 \sin(\delta\phi) \left\{ \int_{-\infty}^{-\Delta} \frac{d\omega}{2\pi} n_F(\omega) \text{Im} \left[ \frac{1}{B(\omega + i\eta)} \right] + \int_{\Delta}^{\infty} \frac{d\omega}{2\pi} n_F(\omega) \text{Im} \left[ \frac{1}{B(\omega + i\eta)} \right] \right\}. \quad (4.139)$$

Here, we rewrite  $B(\omega + i\eta)$  the following way,

$$B(\omega + i\eta) = \Omega(\omega + i\eta) + \Gamma(\omega + i\eta)^2 \sqrt{|\Delta|^2 - (\omega + i\eta)^2}, \quad (4.140)$$

$$\text{with } \Omega(\omega + i\eta) = (|\Delta|^2 - (\omega + i\eta)^2) \left( (\omega + i\eta)^2 - \xi_{d1}^2 - \frac{1}{4}\Gamma^2 \right) + |\Delta|^2 \Gamma_{l1} \Gamma_{r1} \sin^2\left(\frac{\delta\phi}{2}\right). \quad (4.141)$$

Let us have a look at the square root in Eq. (4.140) up to linear order in  $\eta$ ,

$$\sqrt{|\Delta|^2 - (\omega + i\eta)^2} \simeq \sqrt{|\Delta|^2 - \omega^2 - 2i\eta\omega} \quad (4.142)$$

$$= -i \text{sgn}(\omega) \sqrt{\omega^2 - |\Delta|^2}. \quad (4.143)$$

We put the branch cut on the negative real axis here. The number under the square root is slightly imaginary. Since it is now  $\omega^2 > |\Delta|^2$ , we are slightly above or below the branch cut, which depends

on the sign of  $\omega$ . Therefore, when we take the square root, the sign in front of the square root depends on  $\omega$ . In the end, we drop any terms with  $\eta$ , because compared to the expression in Eq. (4.143), they give only small contributions to the imaginary part. Therefore, we expand  $B(\omega + i\eta) \simeq B(\omega)$ , which gives

$$B(\omega) = \Omega(\omega) - i\Gamma\omega^2 \text{sgn}(\omega) \sqrt{\omega^2 - |\Delta|^2}, \quad (4.144)$$

where  $\Omega(\omega)$  is a real number. It follows for the current,

$$J_\infty^{(1)} = \frac{2e}{\hbar} \Gamma_{l1} \Gamma_{r1} |\Delta|^2 \sin(\delta\phi) \left\{ \int_{-\infty}^{-\Delta} \frac{d\omega}{2\pi} n_F(\omega) \text{Im} \left[ \frac{1}{\Omega(\omega) - i\Gamma\omega^2 \text{sgn}(\omega) \sqrt{\omega^2 - |\Delta|^2}} \right] + \int_{\Delta}^{\infty} \frac{d\omega}{2\pi} n_F(\omega) \text{Im} \left[ \frac{1}{\Omega(\omega) - i\Gamma\omega^2 \text{sgn}(\omega) \sqrt{\omega^2 - |\Delta|^2}} \right] \right\}. \quad (4.145)$$

For the integral over the negative spectrum, we put  $\omega \rightarrow -\varepsilon$ , with  $\varepsilon > 0$ . Then we flip the limits for integration and we use the fact that  $\Omega(-\varepsilon) = \Omega(\varepsilon)$ , since it is an even function. After that we simplify put  $\varepsilon \rightarrow \omega$ . For the integral over the positive spectrum we use the relation that for any complex number it is  $\text{Im}[z] = -\text{Im}[z^*]$ . Thus, the current reduces to

$$J_\infty^{(1)} = \frac{2e}{\hbar} \Gamma_{l1} \Gamma_{r1} |\Delta|^2 \sin(\delta\phi) \int_{\Delta}^{\infty} \frac{d\omega}{2\pi} [n_F(-\omega) - n_F(\omega)] \text{Im} \left[ \frac{1}{\Omega(\omega) + i\Gamma\omega^2 \sqrt{\omega^2 - |\Delta|^2}} \right] = \frac{2e}{\hbar} \Gamma_{l1} \Gamma_{r1} |\Delta|^2 \sin(\delta\phi) \int_{\Delta}^{\infty} \frac{d\omega}{2\pi} \tanh\left(\frac{\omega}{2k_B T}\right) \text{Im} \left[ \frac{1}{\Omega(\omega) + i\Gamma\omega^2 \sqrt{\omega^2 - |\Delta|^2}} \right]. \quad (4.146)$$

Let us rewrite the current in the following way,

$$J_\infty^{(1)} = \int_{\Delta}^{\infty} d\omega f(\omega) g(\omega), \quad (4.147)$$

with

$$f(\omega) = \tanh\left(\frac{\omega}{2k_B T}\right), \quad (4.148)$$

$$g(\omega) = \frac{1}{2\pi} \frac{2e}{\hbar} \Gamma_{l1} \Gamma_{r1} |\Delta|^2 \sin(\delta\phi) \text{Im} \left[ \frac{1}{\Omega(\omega) + i\Gamma\omega^2 \sqrt{\omega^2 - |\Delta|^2}} \right]. \quad (4.149)$$

It is then

$$J_\infty^{(1)} = \left[ F(\omega) g(\omega) \right]_{\Delta}^{\infty} - \int_{\Delta}^{\infty} d\omega F(\omega) g'(\omega), \quad (4.150)$$

where  $F(\omega)$  is the antiderivative of  $f(\omega)$ ,

$$F(\omega) = \int d\omega f(\omega) = 2k_B T \ln \cosh\left(\frac{\omega}{2k_B T}\right) + \text{const.} \quad (4.151)$$

We choose the constant to be  $2k_B T \ln(2)$ , which gives a factor 2 in front of the hyperbolic cosine. We do that to be consistent with the result of Beenakker and van Houten. We see that the first term of

the current in Eq. (4.150) vanishes, as  $g(\omega)$  is zero at  $\Delta$  and vanishes at  $\infty$ . Remember that  $\Omega(\omega)$  is real. So, we are left with

$$J_{\infty}^{(1)} = -2k_B T \int_{\Delta}^{\infty} d\omega \ln \left[ 2 \cosh \left( \frac{\omega}{2k_B T} \right) \right] \partial_{\omega} g(\omega). \quad (4.152)$$

We would like to find a relation between  $\partial_{\omega} g(\omega)$  and the derivative of the density of states with respect to the phase difference. In [6] they use a relation for the density of states that depends on the scattering matrix. We will use an expression from [17], which is defined as the change in density of states due to the addition of an impurity to the host conduction electrons. They derive the following equation,

$$\Delta\rho(\omega) = \frac{1}{\pi} \text{Im} \frac{\partial}{\partial\omega} \ln (\det T^R(\omega)), \quad (4.153)$$

where  $T^R(\omega)$  is the  $T$ -matrix which we get from the equation of motion for the retarded Green function of the leads. Equation of motion gives for our one-level system

$$G_{\mathbf{k}\alpha, \mathbf{k}'\alpha'}^R(\omega) = \delta_{\mathbf{k}\mathbf{k}'} \delta_{\alpha\alpha'} g_{\mathbf{k}\alpha}^R(\omega) + g_{\mathbf{k}\alpha}^R(\omega) M_{\text{hyb}}^{(\alpha 1)} G_{d,11}^R(\omega) M_{\text{hyb}}^{(\alpha' 1)\dagger} g_{\mathbf{k}'\alpha'}^R(\omega). \quad (4.154)$$

Here we combined the relation for the Green function for the leads we found in Eq. (4.30) with the relation for the hybridization Green function in Eq. (4.36). We compare this to Eq. (3.11), so one can identify the  $T$ -matrix as follows,

$$T^R(\omega) = T_{\alpha\alpha'}^R(\omega) = M_{\text{hyb}}^{(\alpha 1)} G_{d,11}^R(\omega) M_{\text{hyb}}^{(\alpha' 1)\dagger}. \quad (4.155)$$

Next, the determinant of the  $T$ -matrix is calculated as

$$\det T_{\alpha\alpha'}^R(\omega) = \det \left[ M_{\text{hyb}}^{(\alpha 1)} G_{d,11}^R(\omega) M_{\text{hyb}}^{(\alpha' 1)\dagger} \right] \quad (4.156)$$

$$= \det \left[ M_{\text{hyb}}^{(\alpha 1)} M_{\text{hyb}}^{(\alpha' 1)\dagger} \right] \det [G_{d,11}^R(\omega)] \quad (4.157)$$

$$= \frac{|t_{\alpha 1}|^2 |t_{\alpha' 1}|^2}{D_{11}(\omega + i\eta)}, \quad (4.158)$$

where we used that for the determinant of a matrix it is  $\det [G]^{-1} = \det [G^{-1}]$ . Then we just inserted our definition for the determinant of the dot Green function from Eq. (4.107) and  $M_{\text{hyb}}^{(\alpha n)}$  was defined for the Hamiltonian in Eq. (4.11).

Let us go back to the density of states, Eq. (4.153). We can rewrite the imaginary part as follows,

$$\Delta\rho(\omega) = \frac{1}{2\pi i} \frac{\partial}{\partial\omega} \left[ \ln (\det T^R(\omega)) - \ln (\det T^{R*}(\omega)) \right] \quad (4.159)$$

$$= \frac{1}{2\pi i} \frac{\partial}{\partial\omega} \ln \left( \frac{\det T^R(\omega)}{\det T^{R*}(\omega)} \right) \quad (4.160)$$

$$= \frac{1}{2\pi i} \frac{\partial}{\partial\omega} \ln \left( \frac{D_{11}^*(\omega + i\eta)}{D_{11}(\omega + i\eta)} \right). \quad (4.161)$$

If we use again the definition from above  $B(\omega + i\eta) = D_{11}(\omega + i\eta)E(\omega + i\eta)^2$  and the fact that we can approximate  $B(\omega + i\eta) \simeq B(\omega)$  as in Eq. (4.144), we get  $D_{11}(\omega + i\eta) \simeq D_{11}(\omega) = B(\omega)/E(\omega)^2$ ,

as well as  $D_{11}^*(\omega + i\eta) \simeq D_{11}^*(\omega) = B^*(\omega)/E(\omega)^2$ . This gives

$$\Delta\rho(\omega) = \frac{1}{2\pi i} \frac{\partial}{\partial\omega} \ln \left( \frac{D_{11}^*(\omega + i\eta)}{D_{11}(\omega + i\eta)} \right) \quad (4.162)$$

$$= \frac{1}{2\pi i} \frac{\partial}{\partial\omega} \ln \left( \frac{B_{11}^*(\omega)}{B_{11}(\omega)} \right) \quad (4.163)$$

$$= \frac{1}{2\pi i} \frac{\partial}{\partial\omega} \ln \left( \frac{\Omega(\omega) + i\Gamma\omega^2\sqrt{\omega^2 - |\Delta|^2}}{\Omega(\omega) - i\Gamma\omega^2\sqrt{\omega^2 - |\Delta|^2}} \right). \quad (4.164)$$

Remember that  $\Omega(\omega)$ , Eq. (4.141), is also a function of  $\delta\phi$ . If we put  $a = \Gamma\omega^2\sqrt{\omega^2 - |\Delta|^2}$  and differentiate  $\Delta\rho$  with respect to  $\delta\phi$  we obtain

$$\begin{aligned} \frac{d\Delta\rho}{d\delta\phi} &= \frac{1}{2\pi i} \frac{\partial}{\partial\omega} \frac{d}{d\delta\phi} \ln \left( \frac{\Omega + ia}{\Omega - ia} \right) \\ &= \frac{1}{\pi} \frac{\partial}{\partial\omega} \left( \frac{d\Omega}{d\delta\phi} \frac{-a}{\Omega^2 + a^2} \right) \end{aligned} \quad (4.165)$$

$$= \frac{\partial}{\partial\omega} \left( \frac{1}{2\pi} \Gamma_{l1} \Gamma_{r1} |\Delta|^2 \sin(\delta\phi) \text{Im} \left[ \frac{1}{\Omega(\omega) + ia} \right] \right) \quad (4.166)$$

$$= \frac{\hbar}{2e} \frac{\partial}{\partial\omega} g(\omega). \quad (4.167)$$

Here, we identified our result with  $g(\omega)$ , which we defined in Eq. (4.149). Now, we can plug  $\partial g/\partial\omega = (2e/\hbar)(\frac{d\Delta\rho}{d\delta\phi})$  into Eq. (4.152), which gives the contribution for the current from the continuous spectrum,

$$J_\infty^{(1)} = -\frac{2e}{\hbar} 2k_B T \int_\Delta^\infty d\omega \ln \left[ 2 \cosh \left( \frac{\omega}{2k_B T} \right) \right] \frac{d\Delta\rho}{d\delta\phi}. \quad (4.168)$$

Together with  $J_\Delta^{(1)}$ , Eq. (4.138), which contains the contributions from the discrete spectrum, we get the total current

$$J^{(1)} = -\frac{2e}{\hbar} \sum_{\varepsilon_i > 0} \tanh \left( \frac{\varepsilon_i}{2k_B T} \right) \frac{\partial \varepsilon_i}{\partial \delta\phi} - \frac{2e}{\hbar} 2k_B T \int_\Delta^\infty d\omega \ln \left[ 2 \cosh \left( \frac{\omega}{2k_B T} \right) \right] \frac{d\Delta\rho}{d\delta\phi}, \quad (4.169)$$

which corresponds exactly to the result they found in [6].

#### 4.4.3 Zeeman-split dot levels

When we introduced the system's Hamiltonian, we kept the dot level energies differently for spin up and down. So far we considered only noninteracting dot electrons, for which the energies are spin-independent. Here, we would like to investigate the case of a Zeeman-split dot level. For a small enough magnetic field  $\mathbf{B}$ , the dot level splits into the two levels, where the higher level is occupied by the spin up electron and the lower level by the spin down electron. The corresponding Zeeman Hamiltonian looks as follows,

$$H_{\text{Zeem.}} = -\mu_B g \mathbf{S} \cdot \mathbf{B}, \quad (4.170)$$

where  $\mu_B$  is the Bohr magneton, the Landé  $g$ -factor is closely 2 and  $\mathbf{S}$  is the second-quantized spin operator with the components,

$$S_i = \frac{1}{2} \sum_{\sigma\sigma'} d_{\sigma}^{\dagger} \sigma_{\sigma\sigma'}^i d_{\sigma'}. \quad (4.171)$$

Here, we sum over spin  $\sigma = \uparrow, \downarrow$  and the Pauli matrices  $\sigma^i$  with  $i = x, y, z$  were defined in Eq. (4.12) as  $m^i$  with  $i = 1, 2, 3$ . The  $z$ -component then is  $S_z = \frac{1}{2}(d_{\uparrow}^{\dagger} d_{\uparrow} - d_{\downarrow}^{\dagger} d_{\downarrow})$ . Thus, if we apply a B-field in  $z$ -direction, the Hamiltonian turns to

$$H_{\text{Zeem.}} = -\frac{\mu_B g B_z}{2} (n_{\uparrow} - n_{\downarrow}), \quad (4.172)$$

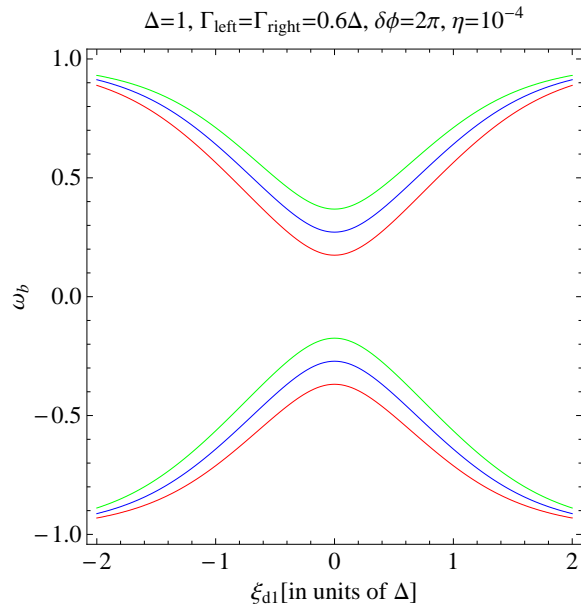
where  $n_{\sigma} = d_{\sigma}^{\dagger} d_{\sigma}$ . Thus, the Hamiltonian of a single dot level with noninteracting electrons  $H_d = \xi_d (n_{\uparrow} + n_{\downarrow})$  becomes under the influence of a Zeeman field,

$$\begin{aligned} H_d^{\text{Zeem.}} &= H_d + H_{\text{Zeem.}} \\ &= \left( \xi_d + \frac{B}{2} \right) n_{\uparrow} + \left( \xi_d - \frac{B}{2} \right) n_{\downarrow}, \end{aligned} \quad (4.173)$$

where we defined the Zeeman energy as  $B = -\mu_B g B_z$ . As we see, the spin-up and spin-down energies are now different in the case of Zeeman splitting. It is thus in our notation for the one-level dot,  $\xi_{d1\uparrow} = \xi_{d1} + \frac{B}{2}$  and  $\xi_{d1\downarrow} = \xi_{d1} - \frac{B}{2}$ , which we can simply plug in the equations for the Green function, Eq. (4.110), to obtain the spectral function, Eq. (4.113). Further, we can determine the current, Eqs. (4.126) and (4.127).

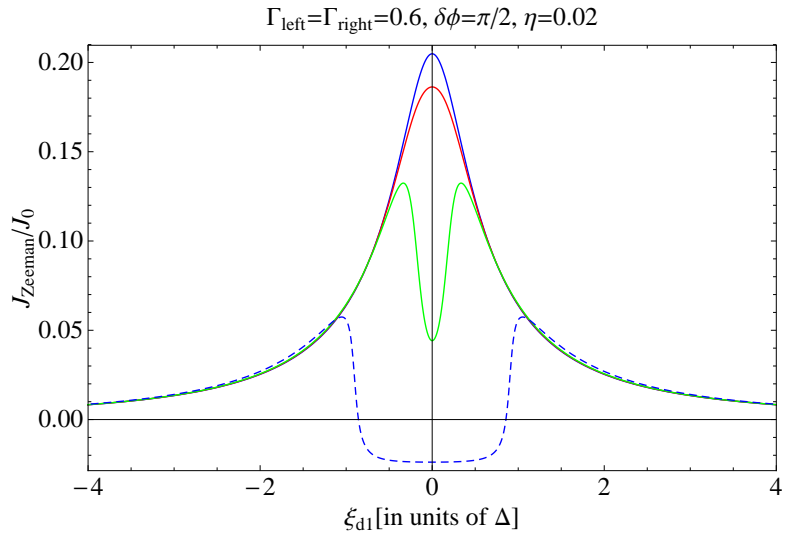
In Fig. 15 we show the bound states with respect to the dot energy  $\xi_{d1}$  for a finite Zeeman field and compare it to the case of zero Zeeman splitting. Thereby, the number of bound states doubles, as the contribution from the spin-up and spin-down level is different. For zero Zeeman fields, this contribution is equal as the spin-up and spin-down level are the same.

Fig. 16 shows the current for different Zeeman energies. The current is the same for  $\pm B$ . If the Zeeman energy is strong enough, there occurs a dip in the current around  $\xi_{d1} = 0$ . If  $B$  is further increased, the current can even become negative, where it is flat with respect to the dot energy. If we have a look at Fig. 17, we see that for big enough Zeeman energy, the Andreev bound state excitation spectrum changes qualitatively. Our results show a connection between the dip in the current and the change in the bound states excitation. This is consistent with the relationship between the supercurrent and the phase dependence of the bound state energies. For small fields, the excitation spectrum is slightly shifted and no dip occurs yet. If we increase the Zeeman field the Andreev bound state excitation spectrum changes qualitatively and there is a dip in the current



**Figure 15:** Bound states vs. dot level for finite Zeeman field. We compare the case of zero field (blue) to  $B = +0.3\Delta$  (red) and  $B = -0.3\Delta$  (green). For a finite Zeeman field the bound states split into a spin-up and spin-down contribution.

around zero level energies. For big enough Zeeman energies, the spectrum moves away from zero energy, thus if we change the dot level energy only slightly the spectrum will not change qualitatively. Therefore, we obtain a flat region for small enough dot level in this case.



**Figure 16:** Current vs. dot level for finite Zeeman field. The figure shows plots for different Zeeman energies,  $B = 0$  (blue),  $B = 0.6\Delta$  (red),  $B = 0.9\Delta$  (green),  $B = 2\Delta$  (dashed). The current for up- and down-spin are equal. For strong enough Zeeman energy, a dip in the current occurs around  $\xi_{d1} = 0$  and it can become even negative.

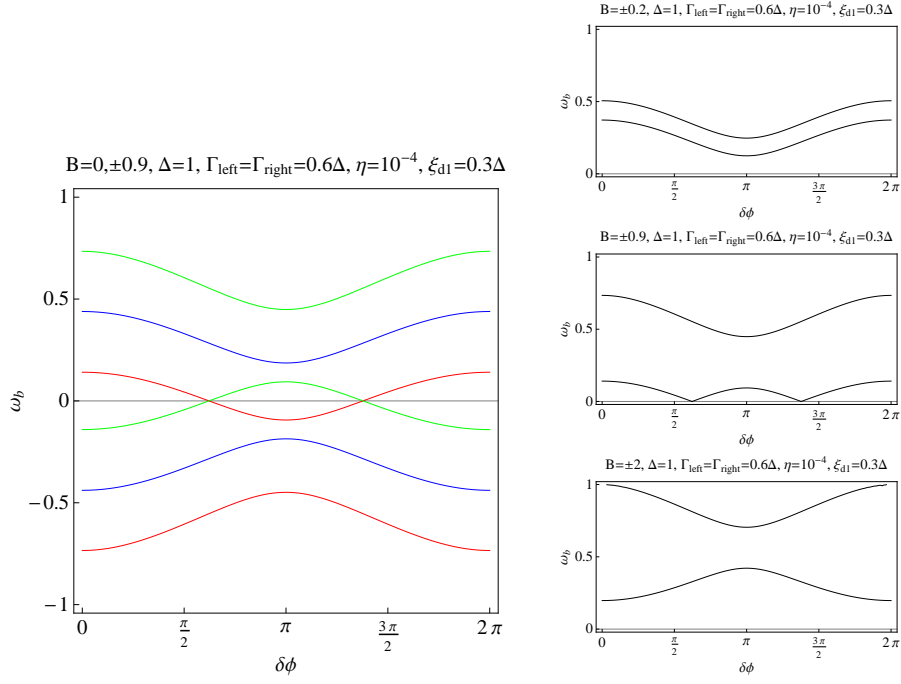


**Figure 17:** Bound states vs. phase difference for finite Zeeman field. **Left:** We show the case of  $B = 0$  (blue),  $B = +0.9\Delta$  (red),  $B = -0.9\Delta$  (green). For finite Zeeman energy the bound states split into a spin-up and spin-down contribution. **Right:** Excitation spectrum (only positive energies) of Andreev bound states for finite Zeeman splitting. In the top panel the Zeeman splitting just causes a shift of the energy levels. In the middle panel the Zeeman splitting causes a qualitative change in the Andreev bound state excitation spectrum. In the lowest panel, the Zeeman energy is so strong that the one excitation line has completely been mirrored.

## 5 Summary & Outlook

We studied the quantum transport of a system containing a noninteracting single-level quantum dot confined between two BCS-superconductors.

First, we introduced the BCS-theory of superconductivity. We saw how the transport between two superconducting leads connected by a nanostructure can be explained by Andreev scattering and the corresponding bound states. Then we introduced the Green function theory for real and imaginary times, as well as times on the contour. The Hamiltonian has been introduced for a general number of dot-levels as well as a general number of leads. It has been rewritten in terms of the Nambu representation to include the particle-hole symmetry. We could derive a general expression for the system's Green functions and supercurrent still for a general number of levels and leads. We did explicit numerical calculations for the case of a one-level dot connected to two superconducting leads. From this we found the Andreev bound states. We saw that they depend on the phase difference as well as the dot level energy and the coupling strength between dot and lead. We found a broadening of the sup-gap states when we added a third, normal lead. The current is a function of phase difference, dot level energy and coupling strength as well. Therefore, one could try to find a relation between current and bound states as well. Furthermore, we could identify our result for the current with the one in [6].

In the end we introduce the Zeeman splitting of the dot level and we explained the relation between the Andreev bound state excitation spectrum and the supercurrent in connection with the strength of the Zeeman field. In future work this could be used to do self-consistent Hartree-Fock calculations for an on-site electron-electron interaction  $U$  by replacing the dot energies by  $\xi_{d\sigma} \rightarrow \xi_d + U\langle n_{d\bar{\sigma}} \rangle$ , as suggested in [14].



## 6 Acknowledgements

I would like to thank my supervisor Jens Paaske for giving me the chance to write my master thesis in Copenhagen and for being always available for questions and discussions. I would also like to thank Felix von Oppen for enabling me to do my master's project outside of Berlin. Furthermore, I thank Gediminas Kirsanskas for helpful discussions. I thank Konrad Wölms for always taking the time to answer my questions and for his great moral support especially through the end phase of my thesis.

Last but not least, I would like to thank my parents, without whom this would not have been possible.



## A Fourier transformation

The time and frequency Fourier transforms we are using here are defined as follows,

$$f(t) = \int_{-\infty}^{\infty} \frac{d\omega}{2\pi} f_{\omega} e^{-i\omega t}, \quad (\text{A.1})$$

$$f_{\omega} = \int_{-\infty}^{\infty} dt f(t) e^{i\omega t}. \quad (\text{A.2})$$

From this we find the special cases,

$$\int_{-\infty}^{\infty} \frac{d\omega}{2\pi} e^{-i\omega t} = \delta(t), \quad (\text{A.3})$$

$$\int_{-\infty}^{\infty} dt e^{i\omega t} = 2\pi \delta(\omega). \quad (\text{A.4})$$

We show here the following relation, which we use in the calculations,

$$A(\omega) = B(\omega)C(\omega) \Leftrightarrow A(t-t') = \int dt_1 B(t-t_1)C(t_1-t'). \quad (\text{A.5})$$

We start from the Fourier

$$\begin{aligned} A(\omega) &= B(\omega)C(\omega) \\ \Leftrightarrow \int \frac{d\omega}{2\pi} e^{-i\omega(t-t')} A(\omega) &= \int \frac{d\omega}{2\pi} e^{-i\omega(t-t')} B(\omega)C(\omega) \\ &= \int \frac{d\omega}{2\pi} e^{-i\omega t} B(\omega) \int d\omega' e^{i\omega' t'} C(\omega') \delta(\omega - \omega') \\ &= \int \frac{d\omega}{2\pi} e^{-i\omega t} B(\omega) \int d\omega' e^{i\omega' t'} C(\omega') \int \frac{dt_1}{2\pi} e^{i(\omega-\omega')t_1} \\ &= \int dt_1 \int \frac{d\omega}{2\pi} e^{-i\omega(t-t_1)} B(\omega) \int \frac{d\omega'}{2\pi} e^{-i\omega'(t_1-t')} C(\omega') \\ \Leftrightarrow A(t-t') &= \int dt_1 B(t-t_1)C(t_1-t'). \end{aligned}$$

## References

- [1] W. Chang, V. E. Manucharyan, T.S. Jespersen, J. Nygård, and C. M. Marcus. Tunneling spectroscopy of quasiparticle bound states in a spinful josephson junction. *arXiv:1211.3954*, Nov 2012.
- [2] Hui Pan and Tsung-Han Lin. Control of the supercurrent through a parallel-coupled double quantum dot system. *Phys. Rev. B*, 74:235312, Dec 2006.
- [3] S. Grap, S. Andergassen, J. Paaske, and V. Meden. Spin-orbit interaction and asymmetry effects on kondo ridges at finite magnetic field. *Phys. Rev. B*, 83:115115, Mar 2011.
- [4] Hong-Kang Zhao and Jian Wang. Zeeman-split mesoscopic transport through a normal-metal–quantum-dot–superconductor system with ac response. *Phys. Rev. B*, 64:094505, Aug 2001.
- [5] H. Shiba. Classical Spins in Superconductors. *Progress of Theoretical Physics*, 40:435–451, September 1968.
- [6] C. W. J. Beenakker and H. van Houten. Resonant josephson current through a quantum dot. *arXiv:cond-mat/0111505v1*, Nov 2001.
- [7] H. Bruus and K. Flensberg. Many-body quantum theory in condensed matter physics. *Oxford University Press, Oxford, U.K.*, 2004.
- [8] C. Timm. Lectures on: Theory of superconductivity (TU Dresden). 2011/12.
- [9] J. R. Schrieffer. Theory of superconductivity. *Advanced Book Program, Westview Press*, 1999.
- [10] A. P. Jauho. Introduction to the keldysh nonequilibrium green function technique. <http://nanohub.org/resources/1877>, Oct 2006.
- [11] H. Haug and A. P. Jauho. Quantum kinetics in transport and optics of semiconductors. *Springer, Berlin*, 1996.
- [12] C. Kittel. Introduction to solid state physics, 5th edition. *New York: John Wiley and Sons, Inc*, 1976.
- [13] T Hecht, A Weichselbaum, J von Delft, and R Bulla. Numerical renormalization group calculation of near-gap peaks in spectral functions of the anderson model with superconducting leads. *Journal of Physics: Condensed Matter*, 20(27):275213, 2008.
- [14] Yu Zhu, Qing feng Sun, and Tsung han Lin. Andreev bound states and the  $\pi$ -junction transition in a superconductor/quantum-dot/superconductor system. *Journal of Physics: Condensed Matter*, 13(39):8783, 2001.
- [15] C. W. J. Beenakker. Universal limit of critical-current fluctuations in mesoscopic josephson junctions. *Phys. Rev. Lett.*, 67:3836–3839, Dec 1991.
- [16] Akira Oguri, Yoichi Tanaka, and Johannes Bauer. Interplay between kondo and andreev-josephson effects in a quantum dot coupled to one normal and two superconducting leads. *Phys. Rev. B*, 87:075432, Feb 2013.

- [17] A. C. Hewson. The kondo problem to heavy fermions. *Cambridge University Press, Cambridge*, 1997.